UNIVERSITÀ DEGLI STUDI DI PADOVA

DIPARTIMENTO DI BIOLOGIA

Corso di Laurea magistrale in Marine Biology

TESI DI LAUREA

The influence of morphology on deep-sea coral distribution: habitat suitability modelling of bamboo corals (Octocorallia: Scleralcyonacea: Keratoisididae) in the NE Atlantic

Relatore: Prof.ssa Carlotta Mazzoldi
Dipartimento di Biologia

Correlatori: Prof.ssa Louise Allcock
University of Galway

Dott.ssa Alexa Parimbelli
University of Galway

Laureanda: Alessia Rizzi

ANNO ACCADEMICO 2022/2023

ABSTRACT

Deep-sea corals are vulnerable marine ecosystems that require conservation and protection actions, but the extreme environment in which they grow makes it difficult to obtain sufficient data to understand their distribution. Species distribution models could be a very effective tool for investigating the occurrence of these benthic communities, but it is necessary to delve deeper into the factors that influence these distributions to obtain accurate and reliable models to be used for management policies. The aim of this study was to investigate the influence of colony morphology on coral distribution, specifically of individuals of the octocoral family Keratoisididae. The software MaxEnt was used to build species distribution models for the three morphologies (unbranched, branched 2D, branched 3D) observed in the NE Atlantic, and then distribution maps were generated in ArcGIS. The models of the three morphologies showed overall a good performance but were not representative of reality, and this might be linked to sampling bias. The occurrence maps obtained from the models highlighted that the three groups have a different distribution pattern, probably linked to the different preferences for the environmental conditions in which to settle. By observing how environmental variables influence the occurrences of the morphologies, it emerged that branched 3D keratoisidids preferred different environmental conditions compared to branched 2D and unbranched bamboo corals, especially with regard to the variables linked to geomorphology (bathymetric position index, rugosity, slope). It has also been demonstrated that the genus *Acanella*, which is part of the branched 3D group, settles in different environmental conditions. Due to the limitations that generally characterize deep-sea investigations, it was not possible to completely accept the initial hypothesis, but the need for further studies regarding the influence of morphology on coral distribution was highlighted.

Keywords: Deep-sea, predictive modelling, Keratoisididae, morphology, SDMs.

TABLE OF CONTENTS

1 INTRODUCTION

The term “deep-sea” is generally applied loosely to describe all the habitats below the epipelagic zone, i.e. below 200 m (NOAA, n.d.). Extreme environmental conditions characterize these habitats. Below 200-500 m light is effectively absent, temperatures are quite constant between -1.8° and 2°C – with the exception of hydrothermal vents, where water can reach 450°C –, pressure increases with depth starting from 20 atm and reaching 1100 atm in the deepest areas, and the availability of food is lower compared to shallower waters (Danovaro *et al.*, 2017). Nonetheless, the deep sea supports a high biodiversity, including representatives of almost all animal phyla (Danovaro *et al.*, 2017; Thistle and Tyler, 2003). This diversity is paramount because it underpins the functions and services provided by the deep-sea ecosystems, including regeneration of nutrients, waste absorption and detoxification, availability of biological and mineral resources, and the scientific knowledge and technological development that accompanies exploration and discovery (Thurber *et al.*, 2014).

Since oceans cover 70% of the planet surface, and 88% of these are deeper than 1000 m, with an average depth of 3800 m, deep marine ecosystems constitute the largest, yet the least explored, biome of Earth (Danovaro *et al.*, 2017; Herring, 2001; Ramirez-Llodra, 2020). It is estimated that only 0.0001% of the whole ocean floor has been investigated through video analysis or physical sampling. The first scientific results were obtained from the expeditions carried out over the last two centuries, when new methods of navigation and new tools for sampling and measurement allowed researches in these hostile environments (Ramirez-Llodra, 2020). Some of these new technologies include Remotely Operated Vehicles (ROVs) and Autonomous Underwater Vehicles (AUVs) used for visual imaging, Conductivity-Temperature-Depth devices (CTDs) that measure physical properties of water, in addition to multibeam echosounders and sidescan sonars for seafloor mapping. The use of ROV systems to investigate deep waters is becoming increasingly popular. These vehicles are unmanned underwater submersibles equipped with high-definition video cameras and a series of physical sensors (e.g., CTDs) (Macreadie *et al.*, 2018; Sward *et al.*, 2019). The data collected by these tools can be used to assess the biodiversity of different habitats, along with information about environmental and geomorphological conditions (Macreadie *et al.*, 2018).

Most deep-sea surveys have focused on benthic environment, because they are easier to investigate than the over 1 billion km^3 volume of the three-dimensional pelagic environment (Ramirez-Llodra *et al.*, 2010). What emerged from these explorations is the vast geomorphological and biological heterogeneity of the deep-sea habitats.

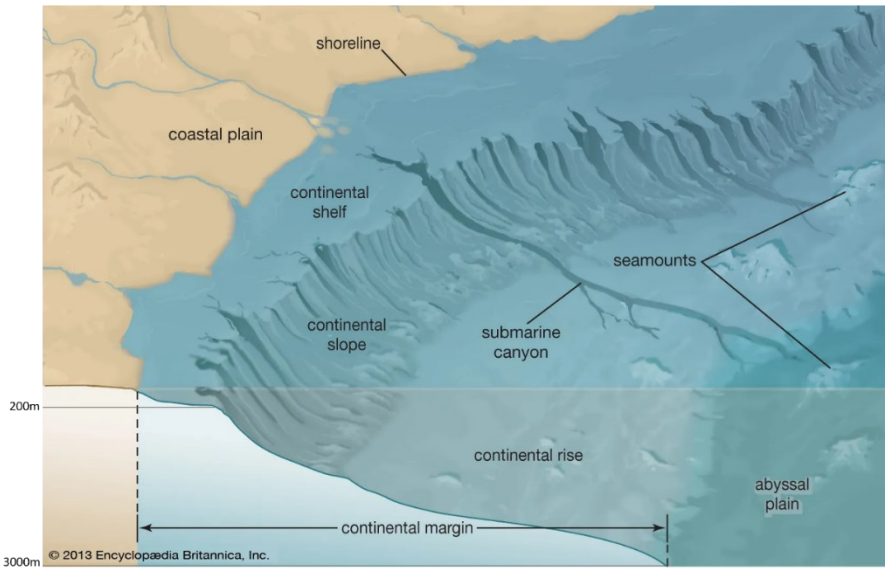

Figure 1. The composition of a continental margin, with the different geological conformations that may be present. Edited image from Encyclopædia Britannica (https://www.britannica.com/science/continental-margin#/media/1/135007/147308)

1.1 Continental margins

Continental margins represent the most geologically diverse settings of seabed, and throughout the planet, they occupy an area of approximately 40 million km^2 (ca. 11-15% of seabed) (Levin and Dayton, 2009; Ramirez-Llodra *et al.*, 2010). They are formed by three main zones, distinguished by the extent and depth to which they descend: continental shelf, continental slope and continental rise (Fig. 1).

The continental shelf extends towards the sea with a gentle slope (on average 0.1°), and extends from the shore to the point defined as "shelf edge" or "shelf break" after which the slope rapidly becomes steeper (Burk and Drake, 2013; Ramirez-Llodra, 2020). On average it has a width of 65-75 km, and coincides with shallow depths of maximum 200-250 m.

The continental slope is that part of the margin that slopes rapidly from the shelf edge towards the ocean bottom (Mouton, 2013; Ramirez-Llodra, 2020). It is considered the margin's steepest portion, with an average slope angle between 3° and 6°, and it can extend more or less in width (5-500 km). Depending on the process of formation of the continental margin, it can reach different depths. Active (endogenetic) margins have a morphology controlled by tectonic and magmatic processes, specifically the ocean floor is so dense that in subduction zones it sinks into the terrestrial crust forming trenches, and therefore reaching depths of 6000-10000 m (Harris and Whiteway, 2011; Hernández-Molina *et al.*,

2008; Ramirez-Llodra *et al.*, 2010). Instead, passive (exogenic) margins are formed following an ocean rift that creates an ocean basin between two parts of the continent, consequently the continental slopes extend up to the abyssal plains, at depth around 1500-4000 m. In these margins, erosion and deposition processes accumulate continental material between the slope and the abyssal plain, generating the continental rise.

The different geological processes that affect this portion of the ocean can lead to the formation of other settings, including seamounts and submarine canyons (Fig. 1). The former are isolated peaks that rise more than 1000 m from the surrounding seabed, while the latter are incisions in the continental shelf and slope created by erosion processes by currents and events such as slumping and submarine landslides (Harris and Whiteway, 2011; Ramirez-Llodra *et al.*, 2010). Both these geological formations are characterized by vertical walls with a more or less steep slope, and are associated with a high biodiversity, especially of corals (Amaro *et al.*, 2016; Robert *et al.*, 2015).

1.1.1 The Irish Continental Margin

The Irish-Scottish Continental Margin is an exogenic margin that extends in the NE Atlantic beyond the Irish coastline over an area of approximately 880,000 km^2, representing one of the largest European seabed territories (Marine Institute, 2022a). Over the last 150 years this region has been extensively investigated through multiple expeditions aboard various vessels (e.g., *HMS Lightning, HSM*

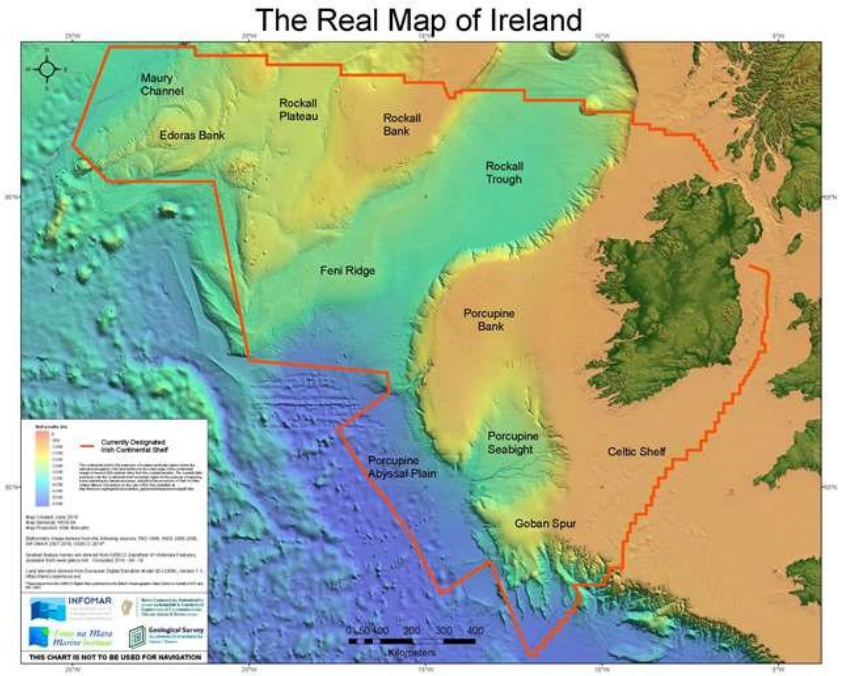

Figure 2. The current designated Irish Continental Shelf, generally referred as the "Real Map of Ireland" (INFOMAR, 2022). Retrieved from https://www.marine.ie/site-area/irelands-marine-resource/real-map-ireland-0.

Porcupine, RV Celtic Explorer, etc.), ROV dives, and seabed mapping campaigns (Morrissey *et al.*, 2023b; Sacchetti *et al.*, 2012). These surveys highlighted a high heterogeneity of benthic environments, including volcanic seamounts, rifted sedimentary basins, and submarine canyons.

Within the Irish margin it is possible to distinguish different geographical areas, characterized by different settings (Morrissey *et al.*, 2023b).

In the northern part that borders the continental shelf off NW Britain, two large banks (Rockall Bank and Porcupine Bank) extend, separated in the middle by Rockall Trough. Rockall Bank is west of the shelf-contiguous Irish Margin, in the same area where the Fangorn Bank volcanic complex is located even further west (Morrissey *et al.*, 2023b; Sacchetti *et al.*, 2012). Rockall Trough is a bathymetric depression approximately 1000 km long and 200-250 km wide, which develops in the north at a depth of 1000-1500 m and continues opening into the Porcupine Abyssal Plain at 3500 m. Sea mountains rise from the seabed in this area, including Rosemary Bank and Anton Dohrn Seamount (Howe *et al.*, 2006). The margin of the eastern Rockall Trough is rich in geological formations, such as canyon systems and escarpments, which characterize the entire north-western edge of Porcupine Bank. South of the latter, the continental margin forms a recess, where the Porcupine Seabight extends. Exploration of this region has highlighted the presence of numerous coral mounds, i.e. complex habitats composed of sediments and biogenic structures, mainly corals of the order Scleractinia (Conti *et al.*, 2019; Morrissey *et al.*, 2023b). Furthermore, the submarine canyon Gollum Channel is located within this embayment.

The Whittard Canyon system is situated in the southernmost region of the Irish Continental Margin. The canyon is composed of four V-shaped branches which converge from the shelf edge towards the flat bottom at 4500 m which then opens in the Biscay Abissal Plain (Amaro *et al.*, 2016).

In all these regions, high biodiversity, especially of corals, has been observed (Morris *et al.*, 2013; Morrissey *et al.*, 2023b; Robert *et al.*, 2015).

1.2 Cold-water corals

The deep-sea ocean floor has always been considered a uniform and undisturbed environment, associated with low biodiversity. The technological progress that has occurred in recent decades has disproved the former ideas, revealing benthic communities with high species richness, especially invertebrates, and a variety of adaptations (Hessler and Sanders, 1967; Rex, 1981; Wolff, 1977). Among the fauna composing deep-sea benthic communities there are corals.

Corals are anthozoan or hydrozoan cnidarians that either secrete calcium carbonate (calcite or aragonite) to build a continuous skeleton, numerous individual sclerites to form an axial column, or that have a black proteinaceous axis (Cairns, 2007). They can occur as single organisms or colonies. A polyp is the living individual of a coral. Polyps have a cylindrical structure where it is possible to identify two tissue layers, ectoderm and endoderm. A gelatinous matrix, called mesoglea, is enclose in the middle between the two layers, where a few specialized cells reside. The body contains a gastrovascular cavity (coelenteron), which opens outwards with a mouth located in the center of a flat oral disc. Tentacles depart from the edge of the oral plate, arranged in one or more rows, and equipped with nematocysts, specialized stinging organelles. Longitudinal tissue septa called mesenteries divide the coelenteron, providing support to the structure of the polyp; these compartments also contain digestive and reproductive cells (Roberts, 2009). Reproduction can be asexual through fragmentation or budding, or sexual with the formation of gametes in the mesenteries and internal or external fertilization. The zygote that is generated develops into a free-swimming larva (Goreau *et al.*, 1979).

Corals are very widespread organisms in the oceans and are found both at shallower depths and at abyssal depths (from 4000 to 7000 m). Below 50 m depth, they are defined as “cold-water corals” (CWC), as they occur in an environment characterized by low temperatures (4-12°C) and dark conditions (Cairns, 2007; Freiwald *et al.*, 2004; Roberts, 2009). Unlike warm-water corals, they lack symbiotic light-dependent algae, and instead feed on particles present in the surrounding water. Little is known about the biology and ecology of CWCs, except that they are characterized by a long life, and therefore slow growth and late maturation, and that with their three-dimensional structure they create complex habitats where it is possible to find many associated species (Bourque and Demopoulos, 2018; Linley *et al.*, 2017; Parimbelli, 2020; Pierrejean *et al.*, 2020). Cold-water corals are hydrozoans of the Stylasteridae family, the hexacorals orders Scleractinia (stony corals) and Antipatharia (black corals), and the subclass Octocorallia (true soft corals) (Fig. 3) (Cairns, 2007; Roberts and Cairns, 2014).

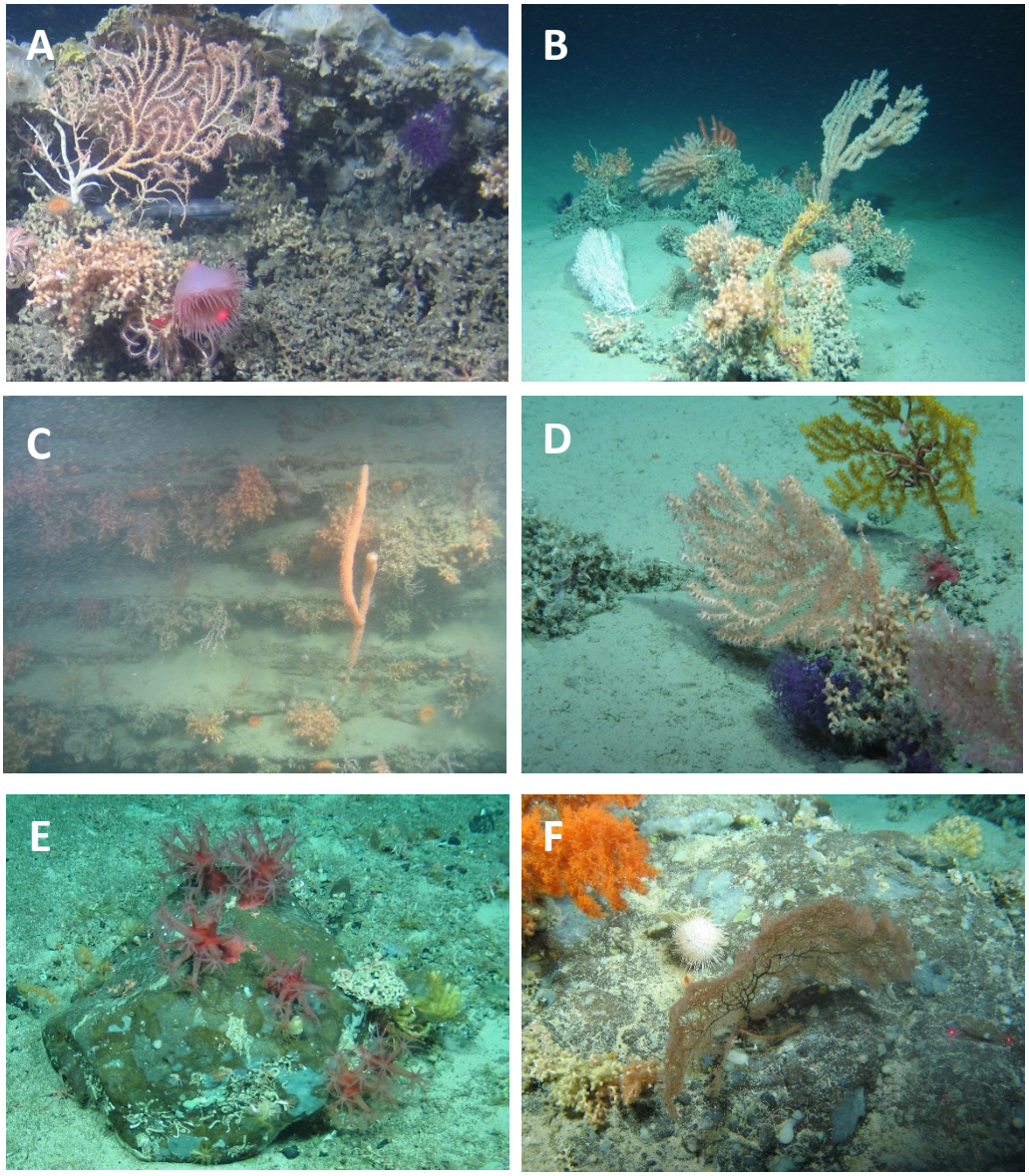

Figure 3. Biodiversity of cold-water corals found on the Irish Continental Margin in the NE Atlantic. Individuals belonging to Octocorallia – Keratoisididae (A, B, C, D), Clavulariidae (A, D), Coralliidae (D, E), Paramuriceidae (B, D, E, F) – and Hexacorallia – Actiniaria (A, C), Antipatharia (E, F), Scleractinia (A, B, C, D). Images taken by ROV *Holland I* during cruise surveys CE13008 (A), CE14009 (B, C), CE17008 (D) and CE21010 (E, F).

1.2.1 Octocorallia: the family Keratoisididae

Octocorals are anthozoans that have polyps characterized by eight mesenteries (8-fold symmetry) from which the same number of tentacles originate, and that typically form colonies where polyps are linked to each other by a tissue called coenenchyma (Freiwald *et al.*, 2004; Watling *et al.*, 2011). Most of these corals, approximately 67% of the total families, are found in the deep-sea, showing

maximum diversity at depths >200 m. With their three-dimensional structure they contribute to the complexity of benthic communities, and provide an important structural role, as they provide shelter for commensal species, harbour eggs and can act as a nursery for juvenile invertebrates (Buhl-Mortensen and Mortensen, 2004; Neves *et al.*, 2020; Parimbelli, 2020; Vecchione, 2019).

The recent phylogenomic analysis carried out by McFadden *et al.* (2022) led to a taxonomic revision of the class Octocorallia, supporting the division of this into two orders: Malacalcyonacea and Scleralcyonacea. The major difference between these two orders lies in the composition of the skeletal axis. Malacalcyonacea are corals that have either a proteinaceous or no skeleton, and they are the species that formerly belonged to the suborders Alcyoniina and Holaxonia, and some taxa previously classified as Stolonifera and Scleraxonia. Instead, the order Scleralcyonacea includes corals with an axis made of calcium carbonate or, alternatively, a fusion of sclerites and calcitic material. It includes the previous order Pennatulacea, many members of the former suborder Calcaxonia, and some taxa previously considered part of Alcyoniina, Stolonifera, Scleraxonia and Holaxonia. Among the taxa of Scleralcyonacea that formerly were included in the suborder Calcaxonia, there is the family Keratoisididae, on which this study focuses.

Keratoisididae Gray, 1870

Keratoisididae are colonial octocorals characterized by a skeletal axis made up of calcareous internodes alternating with sclerite-free proteinaceous nodes, that give a slight flexibility to the structure (McFadden *et al.*, 2022; Saucier *et al.*, 2021). The alternation of nodes and internodes makes the skeleton resemble a bamboo stalk, and for this reason they are commonly called ‘bamboo corals’ (Fig. 4). The colonial structures rise in height with sizes ranging from a few centimetres up to even 3 m (Dueñas *et al.*, 2014; McFadden *et al.*, 2022; Saucier *et al.*, 2021). Growth patterns can be very different, which leads to the observation of various types of morphologies, both unbranched (whip-like), and branched, planar (fan-shaped) or complex (bush/arbuscular) (Fig. 5). They can grow on rocky substrates by attaching to surfaces through a holdfast made of calcium carbonate (Fig. 4) or have a root-like holdfast that anchors to soft sediments. Like all other octocorals, they are long live organisms, with late maturation and slow growth.

Bamboo corals are made up of monomorphic orange-pinkish polyps, which can contract to varying degrees or only the tentacles contract towards the oral disc (Fig. 4). Axial skeleton and polyps are held together by a layer of coenenchyma, the common tissue that covers octocorals. Inside the polyp body and the coenenchyma there are sclerites, which can appear in different shapes (needle, spindle, rod or scale) and be differently oriented along the polyp.

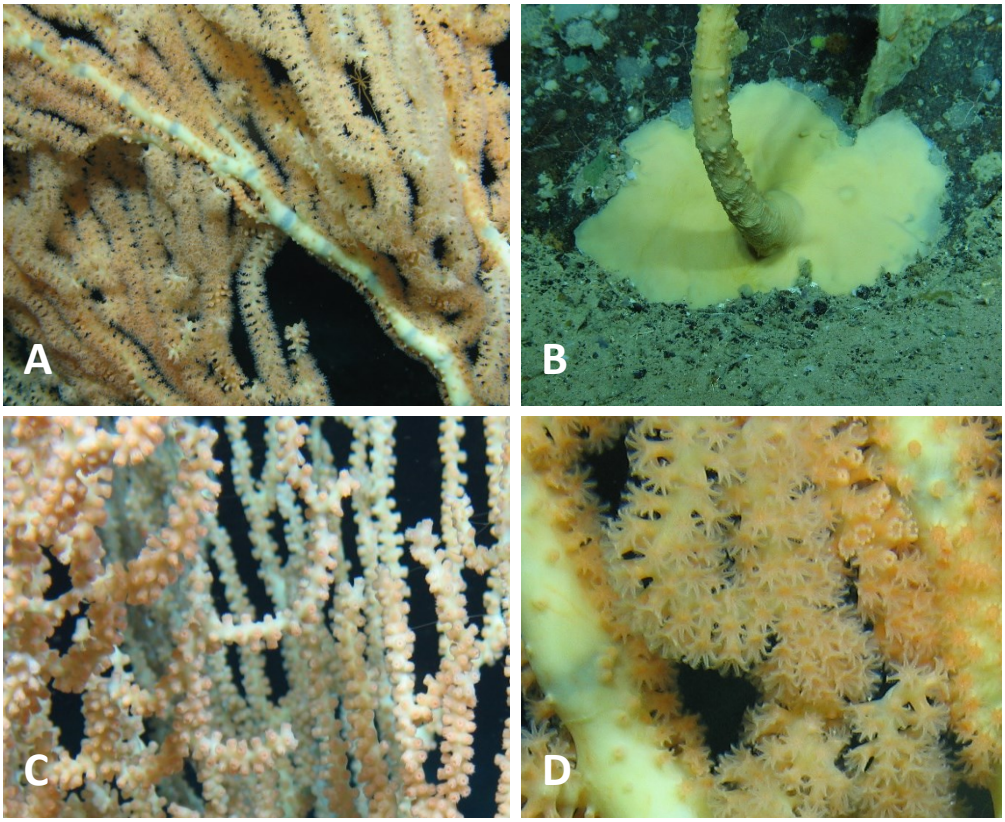

Figure 4. ROV stills showing close-ups of bamboo corals, where it is possible to observe the bamboo pattern of the alternating internodes and nodes on the axial skeleton (A), the holdfast of individuals adhering to rocky substrates (B), contracted and open polyps with their eight tentacles (C, D). Images taken by ROV *Holland I* during the FB11 event of the cruise survey CE21010.

The genera recognized within the Keratoisididae family are *Acanella* (Gray, 1870), *Bathygorgia* (Wright, 1885), *Eknomisis* (Watling & France, 2011), *Isidella* (Gray, 1857), *Jasonisis* (Alderslade & McFadden, 2012), *Keratoisis* (Wright, 1869), *Lepidisis* (Verrill, 1883), *Ortomisis* (Bayer, 1990). These taxa are currently under review, as the branching pattern has always been used as a character to distinguish the various genera, but recent genetic analyses have disproved the congenericity of some individuals (McFadden *et al.*, 2022; Morrissey *et al.*, 2023a; Saucier *et al.*, 2021). In addition, there are many morphologically distinct clades that need to be confirmed as new genera (Morrissey *et al.*, 2022; Watling *et al.*, 2022).

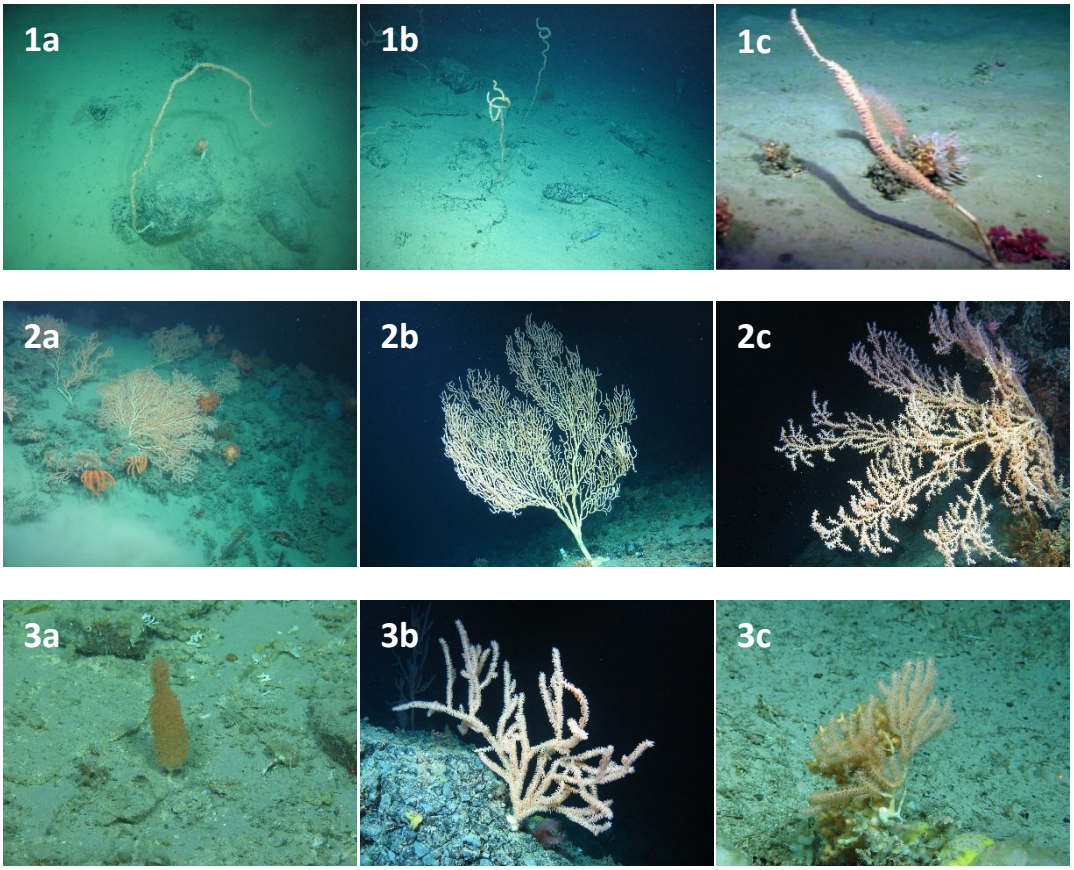

Figure 5. Highlight of the various morphologies found within Keratoisididae families, in particular whip-like (1 a-c), fan shape (2 a-c) and bush/arbuscular shape (3 a-c). Images taken by ROV *Holland I* during different dive events from cruise surveys CE14009 (1c, 2a), CE16006 (2c, 3a), CE18012 (2b, 3b) and CE21010 (1a, 1b, 3c).

Little is known about these corals, as they often inhabit extreme environments, which make it difficult to obtain information and good quality samples. Keratoisidids have a cosmopolitan distribution, and can be found in shallow waters up to 5000 m deep, although a high biodiversity of these corals has been identified in deep-sea environments such as continental slopes, seamounts, submarine canyons, and ridges (Dueñas *et al.*, 2014; Freiwald *et al.*, 2004; Lapointe and Watling, 2015; Watling *et al.*, 2011). Here, they can aggregate to create forests or gardens.

Bamboo corals constitute an important component of deep-sea benthic communities. Like other octocorals with three-dimensional colonial structure, they increase complexity of the ocean floor by modifying particle sedimentation and providing areas for settlement, refuge and niche space (Pierrejean *et al.*, 2020). Specifically, colonies of keratoisidids help to change the flow of water, offering maximum flow and therefore a greater food supply for many filter-feeding organisms, although few commensal species have been directly observed on these

corals (Buhl-Mortensen and Mortensen, 2004; Parimbelli, 2020; Watling *et al.*, 2011). In general, the presence of bamboo corals helps to enhance faunal diversity and ecosystem functioning (Pierrejean *et al.*, 2020).

For their life history traits, their distribution in deep-sea environments and the ecological functions and services they provide, keratoisidid gardens fall within the description given by the Convention on Biological Diversity for identifying ecologically or biologically significant areas (EBSAs) (2008 Decision IX/20 Annex 1) and the description given by the Food and Agriculture Organization of the United Nations (FAO)) for identifying vulnerable marine ecosystems (VMEs). This means that it is essential to know the distribution of bamboo corals on the ocean floor, so as to be able to implement monitoring actions and conservation policies. However, the extreme environments in which these individuals usually grow are very difficult to investigate, and therefore it is necessary to use new methods to survey and define the characteristics of their distribution.

1.3 Species Distribution Models

Establishing where and to what extent deep-sea species are distributed is very difficult. It requires a complete mapping of the areas in which these individuals are found, but the survey of the ocean floor is often limited by costs and logistical problems linked to the difficulty of reaching these environments due to the extreme conditions (depth, pressure, high speed of the currents, etc.) (Feng *et al.*, 2022). In recent decades, it has become very common to use species distribution models (SDMs), also called habitat suitability models (HSMs), to investigate the distribution of deep-sea corals (Bennecke and Metaxas, 2017; Elith and Franklin, 2013; Howell *et al.*, 2011; Reiss *et al.*, 2011; Ross and Howell, 2013; Yesson *et al.*, 2012). This ecological modelling technique quantifies the species-environment relationship, and then applies it to map the distribution of the species considered (Elith and Franklin, 2013; Winship *et al.*, 2020). Like all other modelling techniques, it is necessary to follow a series of steps, which have been described in detail by Guisan and Zimmermann (2000).

Niche theory is generally the basis of SDMs. A niche is a space defined by the conditions, usually environmental, and resources required by a particular species to survive, without reference to geographic space (biotope) (Elith and Franklin, 2013; Hutchinson, 1957). The models are therefore built starting from an ecological concept, from the idea of ranges of patterns and processes that limit the distribution of species. In this initial phase, called model conceptualization, there is the collection of localization data (occurrences) of the investigated individuals and a set of environmental, or even biotic, variables which are thought to influence the presence of these organisms.

The next step is the statistical formulation, or verification, i.e. the choice of a mathematical algorithm to predict the behaviour of the chosen response variable and estimate the model coefficients (Guisan and Zimmermann, 2000). There are several statistical approaches based on different assumptions of species-environment relationship that can be applied when modelling. The formulation of a theoretical model is fundamental, but it must also be accompanied by good input data, appropriate spatial resolution and a robust sampling design. To obtain satisfactory results, statistical approaches and modelling techniques are chosen depending on characteristics of biological and environmental data and the purpose of the study. Traditionally, generalized linear and additive models (GLMs and GAMs) have been used to build SDMs: the assumption behind these techniques is that environmental predictors (X) and the response variable (Y), i.e. species occurrence/abundance, are linearly dependent or linked by a more complex relationship (Elith and Franklin, 2013; Miller, 2010). Recent advances in computing power and machine learning have made a new set of modelling techniques available. Examples of these new methods include regression trees, artificial neural networks, genetic algorithms, maximum entropy methods, and

support vector machines. They are defined 'data-driven' methods, because *a priori* model specification is not required to apply them.

The mathematical model is then applied to the dataset. Adjusting the parameters and constants of the model helps to improve the agreement between the output predictions and the data considered (Guisan and Zimmermann, 2000). This phase called calibration requires a sensitive analysis to identify the most significant parameters for the model. In the case of SDMs, the influence of different environmental variables on the occurrence of species is preliminarily tested, so that explanatory variables ecologically relevant to the hypothesis can be chosen. Subsequently the constants of the mathematical formulations are adjusted to avoid over-fitting and over-smoothing of the model results.

Once the abundance/occurrences of the species are obtained with the modelling technique, it is possible to predict the potential distribution within the modelled area and therefore obtain a distribution map of the species. The probabilities of occurrence obtained from the models are transformed into presence/absence predictions through a threshold, which is selected trying to maximize the performance of the model and at the same time minimize its standard deviation (Liu *et al.*, 2005). The accuracy and reliability of these predictions depends on the goodness of fit and performance of the model. This can be evaluated using various metrics, which in general require the comparison of the predictions with a validation set to define the number of true positive, false positive, false negative and true negative cases predicted by the model (confusion matrix) (Allouche *et al.*, 2006; Elith and Franklin, 2013). Starting from the confusion matrix it is possible to establish the proportion of correctly predicted sites (overall accuracy), proportion of true presences (sensitivity) and proportion of true absences (specificity). Another way to assess the goodness of a model is the receiving operating characteristic (ROC) curve (sensitivity vs. 1 – specificity), where the area under the ROC curve (AUC) indicates the 'fit' of the model to the data. In addition, the true skill statistic (TSS) test can also be calculated (sensitivity + specificity – 1), as it determines how good the model performance is compared to a random prediction.

Model validation is necessary, so that models can be applied outside the datasets used to calibrate them (Winship *et al.*, 2020). Ideally, new independent data should be used, however this is not always possible. When working with deep-sea species the prohibitive costs and logistic problems can prevent new data from being collected. In these cases, cross-validation is implemented: the starting dataset is divided into 'training' and 'test' data, and the former are used to build the model and the latter used to validate it.

1.3.1 Maximum entropy modelling

The maximum entropy (MaxEnt) method developed by Phillips *et al.* (2006) is a modelling technique that has been widely used for species distribution modelling since 2006, the year it was introduced (Elith *et al.*, 2011; Merow *et al.*, 2013). The concept behind this method is to estimate distribution probabilities of investigated species by finding the probabilities that imply the most spread-out distribution, or closest to uniformity (i.e., maximum entropy) (Phillips *et al.*, 2006; Phillips and Dudík, 2008). This assumption makes it possible to work with incomplete information, such as presence-only datasets, because the absences are extrapolated from the background (for this reason, they are defined 'pseudo-absences').

Like other modelling techniques, MaxEnt is based on the ecological theory that independent variables, generally environmental parameters, influence the distribution of a target species (response variable). MaxEnt provides the algorithm that allows this relationship to be quantified by creating a set of transformations for the predictors (Elith *et al.*, 2011; Phillips *et al.*, 2006). These mathematical modifications are called features, and the modelling software calculates a suitable set of them based on six types: linear, product, quadratic, hinge, threshold and automatic. For each of these feature classes, a regularization parameter governs the closeness of the expected distribution probability with respect to the observation data; this value can be modified to smooth and better fit the model. MaxEnt then gives three types of output, raw, cumulative and logistic, that try to give an estimate as close as possible to the probability that a species is present based on the environment (Elith *et al.*, 2011; Phillips *et al.*, 2006; Phillips and Dudík, 2008). The 'raw' output is the set of non-negative probabilities assigned to each pixel in the study area, which are extremely small. 'Cumulative' and 'logistic' outputs are transformation of these raw probabilities. The first one is obtained by cumulatively summing raw output values, that are then rescaled between 0 and 1 to represent the estimated probability of species occurrence. Instead, the logistic output is the transformation of the raw values into probabilities between 0 and 1 through the logistic function. The latter is easier to interpret and use in various types of analysis, so it is the most considered of the three.

The software also carries out a whole series of statistical analyses, useful for evaluating the generated model. Specifically, it calculates ROC curves and analyses the contributions of the variables to the model by running a jackknife test of regularized training gain (Phillips, 2017).

Despite the easy use of the program, and the good results that have been obtained using it in presence-only studies , MaxEnt requires some precautions to be used (Elith *et al.*, 2011; Merow *et al.*, 2013; Radosavljevic and Anderson, 2014; Reiss *et al.*, 2011; Yesson *et al.*, 2012). In particular, the software assumes that the data introduced for calibration and validation are independent and that there is no

sampling bias. It is therefore necessary to carefully choose the input data, providing a good background dataset from which to extract pseudoabsences, and possibly scattered occurrences in the sampling area (Phillips, 2009).

1.3.2 SDMs for deep-sea marine spatial planning

Vulnerable marine ecosystems and ecologically or biologically significant areas, like cold-water habitats, require monitoring, conservation and protection acts, as stated by the Convention on Biological Diversity and as part of the UN Sustainable Development Goals (UN General Assembly, 2015).

In the case of deep-sea habitats, environmental management can be achieved through marine spatial planning, i.e. the imposition of marine protected areas (MPAs), sanctuaries, no-fishing zones, etc. This approach requires accurate and reliable mapping of the occurrences of marine ecosystems, and for deep-sea benthic communities the distribution of these habitats can only be detected through prediction models (Bennecke and Metaxas, 2017; Howell *et al.*, 2022). Despite studies that have highlighted the potential of this tool (Reiss *et al.*, 2011; Ross and Howell, 2013; Yesson *et al.*, 2012 among many others), the use of models in environmental decision making has not become established yet, due to mistrust in the reliability and accuracy of outputs, and the lack of common modelling practices.

Recent studies and workshops have highlighted the necessity of improving the performance of the models by adopting common good practices, using high resolution data, and expanding knowledge of factors influencing species distributions (Araújo *et al.*, 2019; Elith and Leathwick, 2009; Howell *et al.*, 2022; ICES, 2021; Winship *et al.*, 2020).

1.4 Aims and objectives of the study

The aim of this study was to verify the influence of morphology on the distribution of deep-sea corals, using the octocoral family Keratoisididae as representative. This offers further insight into the parameters that determine the presence of corals on the oceanic floor, which is fundamental to obtaining accurate and reliable species distribution models that can be used to inform and improve conservation and protection management of these vulnerable marine ecosystems. To accomplish this task, habitat suitability models were built for the three morphologies that keratoisidids can assume (unbranched, branched 2D and branched 3D), using as dataset the presence records of such specimens in the Irish continental margin in the NE Atlantic.

The main objectives of this thesis were to:

1. Prepare a data subset for each morphological coral form from records of presence of keratoisidids, and project these occurrence data into 200 x 200 m grid cells to extract associated environmental variables from ArcGIS layers.
2. Pre-select the combination of environmental variables that are most important in determining the occurrence of the different morphologies.
3. Build species distribution models for the identified functional groups and map the probabilities of distribution (occurrences) obtained within the study area.
4. Determine whether the three morphologies are distributed differently using various model evaluation metrics and analysing distribution ranges for environmental variables.
5. Compare the distribution of individuals belonging to the Keratoisididae genus *Acanella* with that of other keratoisidids with branched 3D morphology.

2 MATERIALS AND METHODS

2.1 Occurrence data

2.1.1 Video surveys

Video surveys were performed using the remotely operated vehicle (ROV) '*Holland I*' during six research cruises to the NE Atlantic between 2013 and 2021, aboard the Marine Institute vessel *RV Celtic Explorer* (Tab. 1).

Table 1. Summary of *RV Celtic Explorer* surveys

Survey Name	Year	Location	Coordinates range	Depth range (m)	ROV dives
CE13008 – Biodiscovery and Ecosystem Function of Canyons	2013	North Porcupine Bank, Whittard Canyon	54.059 - 48.626 (N) 9.556 - 12.637 (W)	654-2560	16
CE14009 – Ecosystem functioning and biodiscovery at Whittard Canyon	2014	Whittard Canyon	48.467 - 48.885 (N) 9.945 - 10.642 (W)	605-2710	15
CE16006 – Submarine Canyon Ecosystem Services	2016	Whittard Canyon	48.428 - 48.866 (N) 9.941 - 11.048 (W)	702-2100	28
CE17008 – Exploiting and conserving Deep-Sea Genetic Resources: SFI cruise I	2017	Hovland Mounds, Gollum Channel, Belgica Mounds, Whittard Canyon	48.344 - 52.158 (N) 9.565 - 12.451 (W)	790-1830	22
CE18012 – Exploiting and conserving Deep-Sea Genetic Resources: SFI cruise II	2018	North Porcupine Bank	55.648 - 54.027 (N) 9.587 - 13.910 (W)	960-2280	17
CE21010 – Resources of Rockall	2021	Fangorn Bank	55.034 - 55.543 (N) 19.478 - 20.159 (W)	924-1700	13

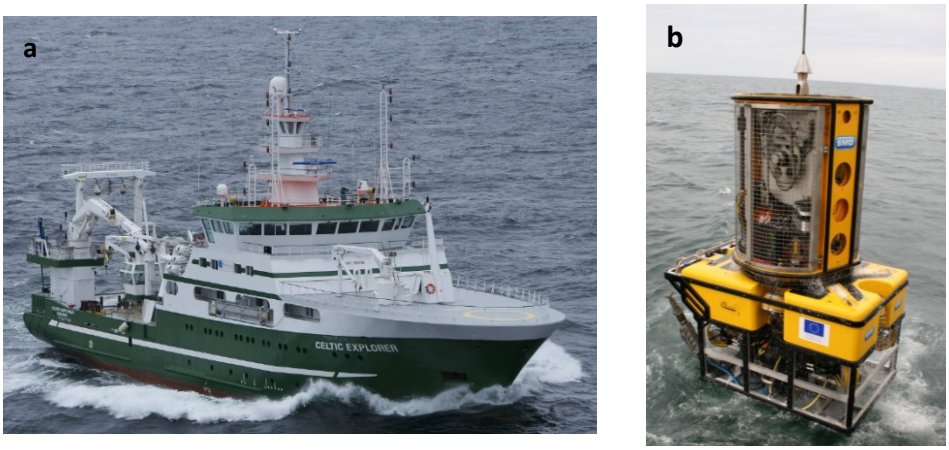

Figure 6. The Marine Research Vessel (RV) Celtic Explorer (a) and Holland I Remotely Operated Vehicle (b). Pictures from https://www.eurofleets.eu/

Holland I is the ROV system developed for the deployment from the *RV Celtic Explorer*, but it can also be transferred to other ships (Fig. 6). It is equipped with a high-definition camera system for videos and stills, supported by powerful

lighting, and with manipulators for both biological and sediment sampling. The entire ROV system was designed to reach depths of 3000 m (Marine Institute, 2022b).

In total, 111 ROV dives were completed in several locations on the Irish Margin, with the majority occurring on the Porcupine Bank, Whittard Canyon system and Fangorn Bank (Fig. 7). During these dives, the ROV generally followed a transect with a constant velocity. When something interesting was glimpsed within the field of view or to the side, a change of trajectory, stops, and close-ups were made, also to allow the collection of fauna and sediment samples for future analysis.

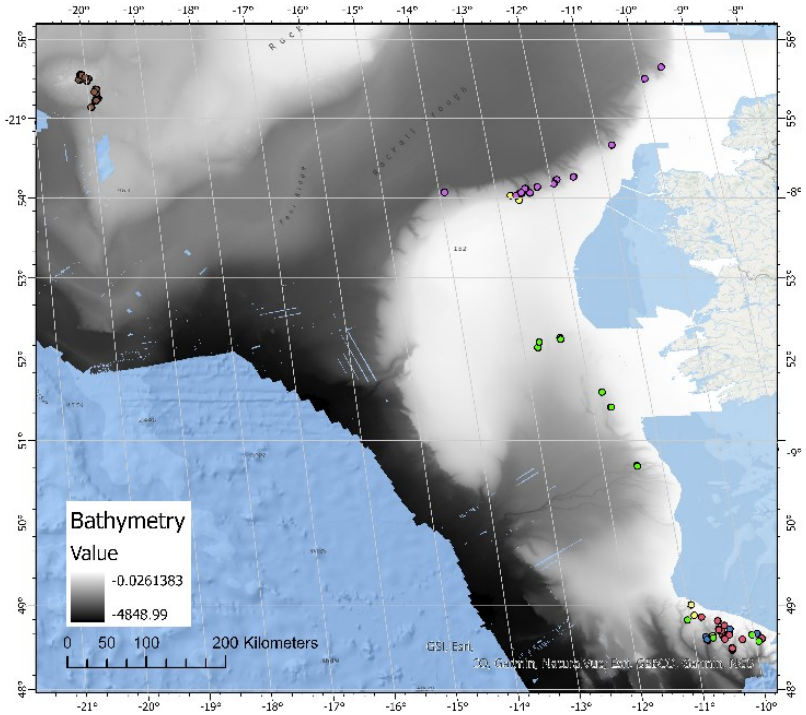

Figure 7. ArcGIS map showing the locations of ROV dives of the cruises in 2013 (yellow), 2014 (blue), 2016 (red), 2017 (green), 2018 (pink) and 2021 (brown). Bathymetry layer from Howell *et al.* (2022)

2.1.2 Video analysis

The video recordings were analysed using the Video Annotation and Reference System (VARS) v. 8.3.1, developed by the Monterey Bay Aquarium Research Institute (MBARI) (Schlining and Stout, 2006). The software was used to annotate the occurrence of corals and other organisms in the videos, along with the time of observation.

The observed specimens were annotated and identified at the lowest taxonomic level, based on an in-house species identification catalogue of Irish deep-water organisms built over the years. Due to the difficulty in identifying organisms from

video data, it was not possible to determine all organisms to species level. For this reason, morphospecies (i.e. individuals with similar appearance to which the taxonomic level shared by both is attributed) were identified and annotated (Howell *et al.*, 2010).

Since the cruise expeditions were carried out years apart, the video recordings were examined at different times and by different analysts. However, consistency was ensured by following some common guidelines:

- During the observation of the video tapes, only organisms within the field of view illuminated by the ROV's light were annotated, while those in dim light or on the sides were not considered until they were lit.
- For each specimen observed, or colony as in the case of corals, a single annotation was made. However, when there were more than ten individuals of the same species in the field of view, they were described by a single annotation accompanied by a "+" sign in the notes.
- If the organisms were too difficult to identify, e.g. the image was too blurred, the individuals were too small or had characteristics attributable to more than one phylum, or the ROV was moving too quickly, they were annotated as "Indeterminate", adding a brief description in the notes to facilitate their recognition on the screen later.
- The organisms collected by the ROV were noted only at the time the collection process began, and a single annotation remained even if the specimen broke or if the acquisition required multiple steps. A "collected" note was added to the identification of the acquired individual, with the corresponding 'specimen number' (distinctive number attributed to each sample collected) that easily connects the sample to the place and time of collection.
- Along with the organisms, the substrate composition was recorded at the beginning of each video, and then every 30 minutes and whenever it visibly changed. The three main categories of substrate are mud, rock and coral rubble, but in some cases combinations of these types or special cases of them (e.g., rock walls, boulders, etc.) can be observed (Fig. 8).

Following the video analysis, the observations were downloaded into CSV files using the VARS "Query" application, which allowed the annotation of each morphotype to be linked with its taxonomic information. The different datasets generated for each survey were then merged into a single file.

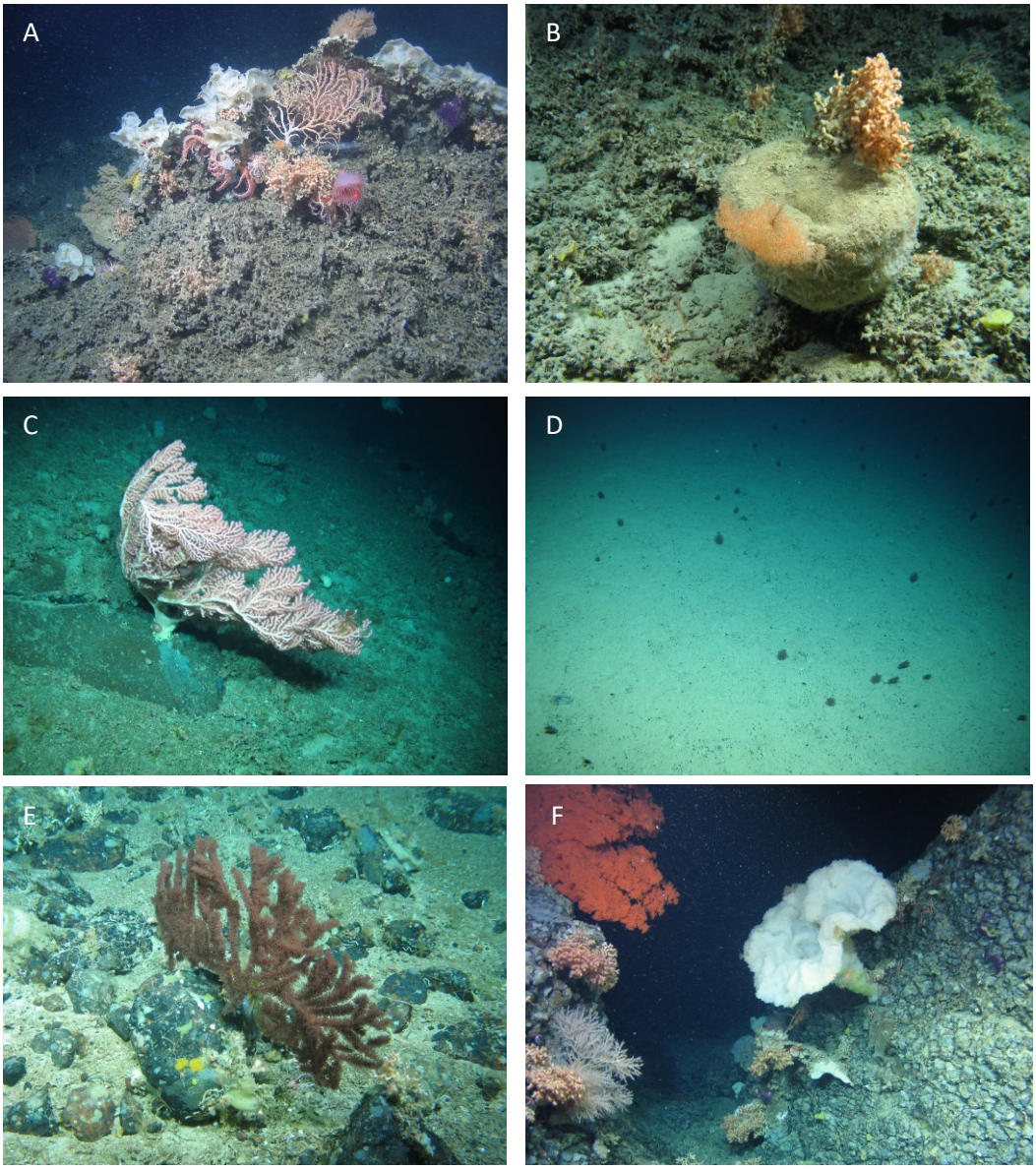

Figure 8. Types of substrates observed in the cruise expeditions: (A) coral rubble; (B) mud and coral rubble; (C) mud and rocks, with coral rubble; (D) mud; (E) mud and rocks; (F) rock wall. Images taken by *Holland I* ROV during the cruise's expeditions CE18012 and CE21010.

2.1.3 Data manipulation

The occurrence dataset was linked to the coordinates and depth at which the morphotypes were annotated. Positioning data were retrieved from the USBL system which consisted of transponders on the ROV communicating with those on the drop-down keel of the ship, with the signals processed using a sound velocity profile generated by a CTD cast prior to ROV deployment. To obtain latitude and longitude for every second of each transect, USBL positioning data were smoothed and splined through the Ocean Floor Observational Protocol (OFOP) software (Huetten and Greinert, 2008). The 'pandas' tool in Python was then used to link

occurrence and splined positioning data in order to assign to each annotation the coordinates and depth where the organisms were observed.

Since many dive events were conducted at the same locations as others, it was necessary to ensure that there were no double records of the same organisms. To do so, a “code transect” number was attributed to each dive to distinguish the various transects explored. By plotting the dataset with all the annotations in ArcGIS, it was possible to identify through this code the dives that partially followed the same transect or that intersected. A second numerical code, called “group transect”, was attributed to the events, so that intersected dives had the exact same group transect number (refer to Table 1 of Appendix A).

As this study focuses on members of the family Keratoisididae (clades illustrated in Appendix B), a subsample containing morphotypes belonging to this family was extracted and used for the modelling study. The Keratoisididae records were further dived into three groups depending on their morphology (Fig. 9):

(1) Unbranched, which are characterized by a single branch, resembling a stick or a whip;
(2) Branched 2D, which are the planar bamboo corals, generally called fan-shaped;
(3) Branched 3D, which branch in every direction, taking on a bush or tree shape.

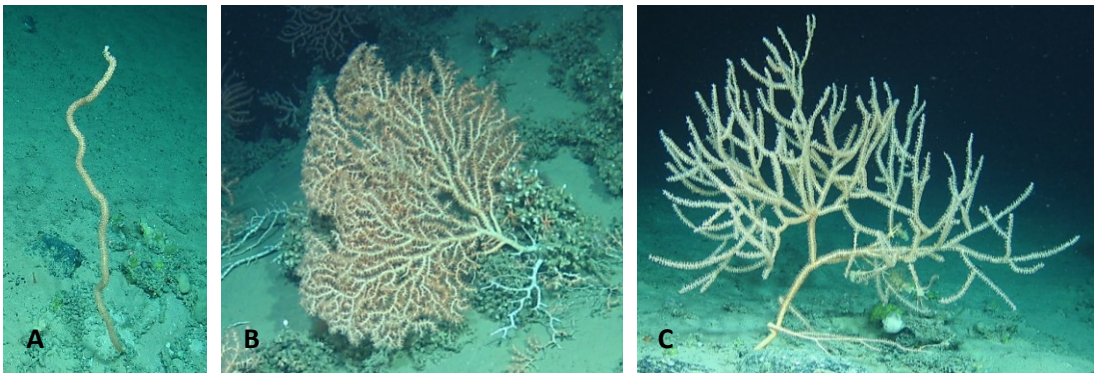

Figure 9. The three different morphologies occurring in the family Keratoisididae: (A) unbranched, (B) branched 2D, and (C) branched 3D.
Images taken by ROV *Holland I* during the dive events PG1 and FB2 from the cruise CE21010 (respectively, A, C), and event 25 from CE14009 (B).

The distinction in the three different morphologies was made following the studies of Morrissey *et al.* (2022) and Dueñas *et al.* (2014) (Tab. 2), and comparing the individuals to the pictures reported in the species identification guide.

Table 2. Keratoisididae genera and morphotypes used for the video identification, and corresponding morphologies.

Morphotype	Colony shape	Reference
Genus *Acanella*	Branched 3D	Morrissey et al. (2022); Dueñas et al. (2014)
Genus *Eknomisis*	Branched 3D	Morrissey et al. (2022); Dueñas et al. (2014)
Genus *Isidella*	Branched 2D	Dueñas et al. (2014)
Genus *Jasonisis*	Branched 2D	Dueñas et al. (2014)
Genus *Keratoisis*	Unbranched	Dueñas et al. (2014)
Genus *Lepidisis*	Unbranched	Dueñas et al. (2014)
Clade B1	Unbranched or Branched 2D	Morrissey et al. (2022)
Clade C1	Unbranched	Morrissey et al. (2022)
Clade D1	Branched 2D or Branched 3D	Morrissey et al. (2022)
Clade D2	Branched 3D	Morrissey et al. (2022)
Clade F1	Unbranched	Morrissey et al. (2022)
Clade I1	Branched 3D or Unbranched	Morrissey et al. (2022)
Clade J3	Branched 2D	Morrissey et al. (2022)

2.2 *Environmental variables*

Ten environmental variables were selected based on their biological relevance and availability: bathymetry, broad and fine bathymetric position indices (BBPI and FBPI), curvature (overall, plan and profile), rugosity, salinity, slope and temperature.

Raster files for these parameters were available from previous studies (Howell *et al.*, 2022; Ross and Howell, 2013). Bathymetric data were in part obtained from the General Bathymetric Chart of the Oceans (GEBCO) and part from additional high-resolution multibeam bathymetry data retrieved from sidescan sonar surveys (Howell *et al.*, 2022). The resulting layer was then resampled at a resolution of 200 x 200 m grid cells (Fig. 10). Bathymetric position indices, curvature, rugosity and slope layers were generated from bathymetry using ArcGIS Benthic Terrain Modeler extension (Walbridge *et al.*, 2018). Bottom temperature and salinity information derived from CTD data was used to build generalize additive models (GAMs) and create raster grids (Guinan *et al.*, 2009; Howell *et al.*, 2022; Ross and Howell, 2013). These layers were then projected in ArcGIS and trimmed to the same extent as the bathymetry.

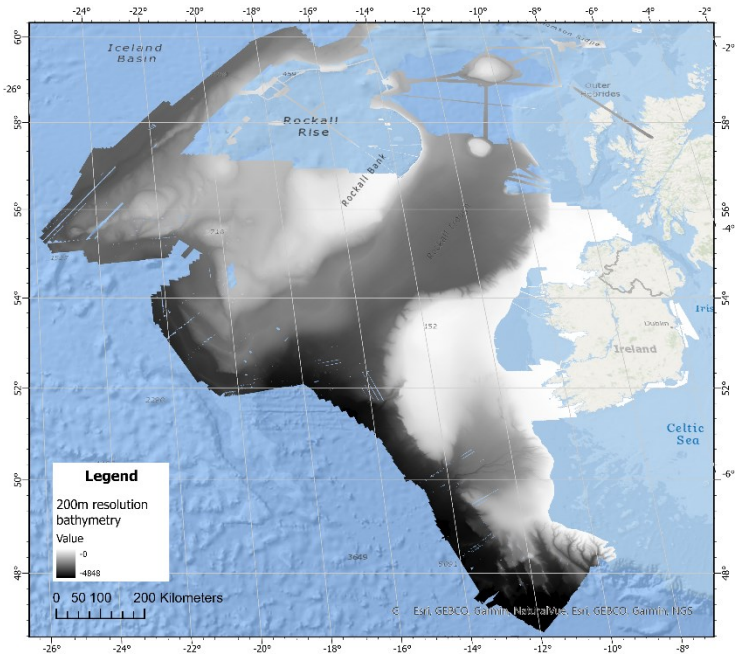

Figure 10. Bathymetry layer at resolution 200 x 200m, derived from Howell *et al.* (2022). Visualized in ArcGIS Pro.

2.3 Modelling

Six models were trained: (1) entire family, (2) unbranched morphology, (3) branched 2D morphology, (4) branched 3D morphology, (5) branched 3D morphology without *Acanella*, and (6) genus *Acanella*. In the literature the genus *Acanella* has shown a specific preference for a certain type of habitat, quite different from that preferred by the other bush bamboo corals (Robert *et al.*, 2015; Saucier *et al.*, 2017).

To ensure that all environmental variables were weighted evenly in the models, the occurrence data of each dataset considered was reduced to one point per cell in ArcGIS Pro v3.1. A presence (1) was assigned to each cell in which at least one individual belonging to the group of interest was observed, otherwise, or in the case of unexplored cells, a pseudoabsence (0) was assigned (Howell *et al.*, 2022; Ross and Howell, 2013). In addition, a single presence point was randomly selected for each transect, and same for the absences in absence transects. This reduction to a single point per transect was undertaken to avoid a potential spatial autocorrelation effect within the models.

Environmental variable data were then extracted through ArcGIS 'Extract multi values to points' tool from the respective layers, so that each presence/absence was associated with a specific set of environmental values.

The models were built using presence-only data, as all the absences were obtained from a lack of observation of the targeted morphology class. The maximum entropy (MaxEnt) modelling developed by Phillips *et al.* (2006) has been found to have the highest performance for this type of data (Elith *et al.*, 2006), and was thus used throughout the study. MaxEnt is a software that has been widely used to model species distributions since it was introduced in 2006 (Elith *et al.*, 2011). Through the algorithm behind this software, the target probability is estimated as the probability distribution of maximum entropy, i.e. as if the data are close to being uniform, and this is why it is possible to work with presence-only records (Phillips *et al.*, 2006; Phillips and Dudík, 2008).

Multi-model selection method was applied to ensure that the variables included in the model were relevant for the study (Burnham *et al.*, 2011; Elith and Leathwick, 2009). Within a set of models, this method selects the model that minimize the loss of information in approximating reality, i.e. the closest to full reality. To avoid adding noise to the models, the correlated variables were first identified, applying the rule that $|r| > 0.7$ characterizes a covariance. Then, GAMs (gam, K = 4, gamma = 1.4; Kim and Gu, 2004) were built in R studio with the 'mgcv' library (Wood, 2017) for all the variables and combinations of non-correlated variables, and the corrected Akaike information criterion (AICc) was used to choose which permutation gave the best model (Burnham *et al.*, 2011).

Species presences linked to the pre-selected environmental predictors for each functional group were used as input and modelled in MaxEnt v.3.4.4. Following the protocol outlined in Ross and Howell (2013), some preliminary models were first tested to reduce over-fitting and over-smoothing (Phillips and Dudík, 2008). Specifically, different combinations of parameters were trialled, including the feature classes (linear, quadratic, product, hinge and threshold) and the regularisation parameter. For the probability functions, linear, quadratic and product features were maintained in all models, while several arrays of automatic, hinge and threshold features were tested to find which of those gave the highest performance to the models. In particular, for the family Keratoisididae, branched 3D morphology and genus *Acanella*, all the three features were deselected; for unbranched and branched 3D without *Acanella* morphologies, autofeatures and hinge features were not selected; for branched 2D hinge and threshold features were not selected. As regards regularisation parameters, a series of values (0.001, 0.01, 0.1, 0.5 and 3) were initially tested and then the value (to 3 decimal places) that most minimized the AICc value of the models was found with an iterative procedure (Burnham and Anderson, 1998; Howell *et al.*, 2022) (see Table 1 of Appendix C).

2.4 *Model evaluation*

For the evaluation of the models, the procedure already implemented by Ross and Howell (2013) and Howell *et al.* (2022) was followed. Therefore, data were manually partitioned (70/30 split) in R v. 4.3.1, but checking that the transects felt into either a training or testing data set to avoid validation of the same transect with a within-transect testing point (Howell *et al.*, 2011). Data were split ten times, obtaining ten sets of training and test for each functional group considered. New random partitions were made until the training and test data set had prevalence within a range of <±1% compared to that of the full data set.

Ten new models were built for each functional group, and then they were evaluated using the 'PresenceAbsence' package in R (Freeman and Moisen, 2008). The area under the receiver operating curve (AUC) was calculated for the full models and each partition, and also thresholding techniques were employed to assess model performance (Howell *et al.*, 2022; Ross and Howell, 2013). As suggested by Liu *et al.* (2005), three thresholding techniques were used: (1) maximization of Cohen's Kappa (MaxKappa) to measure the overall performances, (2) sensitivity-specificity sum maximization (MaxSens+Spec) to find the true skill of the models, and (3) predicted prevalence and observation equality (PredPrev=obs) to estimate prevalence. The thresholds for each model were selected looking at the average of three widely used indices (sensitivity, specificity and PCC), and depending on which technique maximized the model performance but at the same time minimized the standard deviation.

In addition, using the code developed by Karlsson (2019), true skill statistic (TSS) was calculated for each trained (TSS_{train}) and tested (TSS_{test}) model to assess their transferability outside the dataset. The averages of the TSS_{test}/ TSS_{train} ratios were used to determine the degree of overfitting of the models. The closer this mean is to 1, the less overfitted the model is, i.e., the greater its transferability (Allouche *et al.*, 2006; Parimbelli, 2023)

MaxEnt program can also run Jackknife tests of variable importance, to determine the variables that contributes most to the model. By selecting this option, several models are generated: one with all the pre-selected variables, one excluding each variable in turn and running a model with the remaining variables, and one using each variable individually (Phillips, 2017). The results are then plotted in a bar chart.

2.5 *Differences in predicted distributions*

The probabilities of presence calculated in MaxEnt for each functional group were uploaded in ArcGIS as raster grids. The data were transformed to predicted presence/absence by designing a binary layer with only values above the threshold (Liu *et al.*, 2005). The relative probability data produced from the maps from the ten training and test partition data sets were used to create a standard deviation layer (Howell *et al.*, 2022; Ross and Howell, 2013). In addition, the results of the multivariate environmental similarity surface (MESS) analysis performed by MaxEnt were output as a layer used to create a mask to keep only the reliable predictions (Elith *et al.*, 2011).

To better understand the maps obtained, the distributions by the pre-selected environmental predictor were compared among the six functional groups, first visually generating boxplots with the R package 'ggplot2' v 1.0.0 (Whickam and Winston, 2016), then statistically applying a comparison test. To decide which type of comparison test to use, the condition of normality was assessed by generating Q-Q plots for each variable for all six functional groups. Since the distributions were not normal (results in Appendix D), it was decided to use the Kruskal-Wallis test (Kruskal and Wallis, 1952), a non-parametric test that determine whether there are significant differences between the multiple groups (McKight and Najab, 2010). Multiple comparisons increase the probability of incurring a Type I error (false positive), so it is necessary to accompany them with a correction method. In this case a Bonferroni correction was applied, which makes the level of significance for each individual test more rigorous, maintaining an overall acceptable Type I error rate across all comparisons (Weisstein, 2004).

The null hypothesis tested by Kruskal-Wallis test is that all the medians of all groups are equal; consequently, if the p-values are lower than 0.05 – the commonly chosen level of significance – rejection of the hypothesis implies that there are significant differences between the compared distributions. P-values were therefore calculated using the 'PMCMRplus' package v 4.3 in R (Pohlert, 2018). Since the annotations for the three morphologies were extracted from the Keratoisididae dataset, and branched 3D without *Acanella* and genus *Acanella* were subset from branched 3D dataset, these two broader groups were excluded from the analysis, because the requirement of independent data necessary to perform the statistical test was not met.

With the Kruskal-Wallis test it is only possible to establish whether there are significant differences in the distributions between the multiple groups considered; a *post hoc* test is necessary to identify the pair of groups that are differently distributed (Dinno, 2015). A pairwise comparison was therefore performed; specifically Dunn's test (Dunn, 1964) was applied using the R package 'dunn.test' v 1.3.5 (Dinno, 2017). With this test, significant differences are identified by p-values < 0.05, as it is necessary to reject the null hypothesis that

there are no differences between the two compared groups (Dinno, 2015). Again, since Dunn's test is also a multiple comparison test, the Bonferroni correction method was applied to it within the R code.

3 RESULTS

There were 60 sampling locations explored through transects during the diving events, which covered an area of the NE Atlantic Ocean enclosed in 486 200x200m grid cells. The data considered to build the models for the different morphologies of the family Keratoisididae were a small portion of the dataset composed of 134870 organisms annotated from the ROV videos (Tab. 3).

Table 3. Number of annotations, cells with at least 1 presence and transects with at least 1 presence for each functional group considered.

	Annotations	Cells with at least 1 presence	Transects with at least 1 presence
Family Keratoisididae	3947	210	40
Unbranched Keratoisididae (stick/whip)	531	71	26
Branched 2D Keratoisididae (fan shape)	561	64	26
Branched 3D Keratoisididae (bush shape)	2852	190	39
Branched 3D Keratoisididae, no *Acanella*	932	99	34
Genus *Acanella*	1920	141	32

3.1 Variable pre-selection

Pairs of variables with absolute values higher than 0.7 in the correlation matrix (Tab. 4) were considered correlated and excluded from the selection of variables. Specifically, a high correlation was found between depth and temperature, BBPI and FBPI, curvature and plan curvature, curvature and profile curvature, FBPI and profile curvature, rugosity and slope, salinity and temperature.

Table 4. Correlation matrix for the environmental variables.
The cells highlighted in red show absolute values higher than 0.7, and so the correlation between the two variables.

	Depth	BBPI	Curv	FBPI	PlanCurv	ProfCurv	Rug	Sal	Slo	Temp
Depth	1	0.019582	0.052877	0.058945	0.00415	-0.07787	-0.23362	0.36481	-0.24956	0.859416
BBPI	0.019582	1	0.534061	0.813478	0.426367	-0.49308	-0.09512	-0.1393	-0.06509	-0.02095
Curv	0.052877	0.534061	1	0.848538	0.825538	-0.90251	-0.04468	-0.05157	-0.0162	0.028164
FBPI	0.058945	0.813478	0.848538	1	0.68135	-0.78043	-0.04714	-0.10934	-0.03211	0.015282
PlanCurv	0.00415	0.426367	0.825538	0.68135	1	-0.50202	-0.0571	-0.07417	-0.01729	-0.01804
ProfCurv	-0.07787	-0.49308	-0.90251	-0.78043	-0.50202	1	0.024902	0.022436	0.01163	-0.05693
Rug	-0.23362	-0.09512	-0.04468	-0.04714	-0.0571	0.024902	1	0.227534	0.940401	-0.06471
Sal	0.36481	-0.1393	-0.05157	-0.10934	-0.07417	0.022436	0.227534	1	0.262839	0.751903
Slo	-0.24956	-0.06509	-0.0162	-0.03211	-0.01729	0.01163	0.940401	0.262839	1	-0.05484
Temp	0.859416	-0.02095	0.028164	0.015282	-0.01804	-0.05693	-0.06471	0.751903	-0.05484	1

The combination of variables with the lowest corrected AICc value was selected for each functional group considered. Except for branched 3D Keratoisididae without genus *Acanella*, the variables selected for the final models were quite similar (Tab. 5 – for AICc values see Table 2 of Appendix C). The combination for unbranched and branched 2D Keratoisididae was the same, whereas for the entire family of bamboo corals, FBPI was selected instead of BBPI. For branched 3D Keratoisididae and the genus *Acanella*, BBPI and temperature were still selected as important, but together with rugosity instead of slope. The variables selected for the morphology branched 3D without *Acanella* were bathymetry, rugosity and salinity.

Table 5. Relevant variables selected through GAMs for each of the modelled functional group.

Variables	Functional Group					
	Keratoisididae	Unbranched	Branched 2D	Branched 3D	Branched 3D (no *Acanella*)	*Acanella*
Bathymetry					X	
BBPI		X	X	X		X
Curvature						
FBPI	X					
Plan Curvature						
Profile Curvature						
Rugosity				X	X	X
Salinity					X	
Slope	X	X	X			
Temperature	X	X	X	X		X

3.2 Model performance and transferability

For all the functional groups, the preferred thresholding method was MaxKappa and the values ranged from 0.44 found for the family Keratoisididae to 0.76 of the branched 2D bamboo corals (Tab. 6).

Table 6. Thresholding methods and threshold values selected for the six functional group.

Functional Group	Thresholding method	Threshold value
Family Keratoisididae	MaxKappa	0.44
Unbranched Keratoisididae	MaxKappa	0.62
Branched 2D Keratoisididae	MaxKappa	0.76
Branched 3D Keratoisididae	MaxKappa	0.55
Branched 3D Keratoisididae (no *Acanella*)	MaxKappa	0.585
Genus *Acanella*	MaxKappa	0.64

Considering the AUC values, the predictions were better than random (Tab. 7) (AUC > 0.5). The models with the best performance, which can be defined as "good", were for morphologies unbranched (AUC = 0.892) and branched 3D without *Acanella* (AUC = 0.882) (Fig. 11b, 11e). Branched 2D and genus *Acanella* models gave AUC scores moderately good (respectively, AUC = 0.732 and AUC = 0.706) (Fig. 11c, 11f). Models for the family (AUC = 0.642) and branched 3D Keratoisididae (0.663) showed poor performance (Fig. 11a, 11d).

Looking at the averages of TSS_{test}/ TSS_{train} ratios (Tab. 7), the models with the worst performance were actually those that better represent reality, while the 'good' models showed overfitting. The highest accuracy was found for the family Keratoisididae (TSS_{test}/ TSS_{train} = 0.890) and the morphology branched 3D (TSS_{test}/ TSS_{train} = 0.789). The morphologies unbranched and branched 3D without *Acanella* displayed low transferability (respectively, TSS_{test}/ TSS_{train} was 0.207 and 0.231); for the branched 2D Keratoisididae it was slightly better (TSS_{test}/ TSS_{train} = 0.478). Differently, the model for the genus *Acanella* could be considered the best one, because it showed both a pretty good performance and a high accuracy (TSS_{test}/ TSS_{train} = 0.971).

Table 7. Area under the receiver operating characteristic curve (AUC) scores and TSS_{test}/ TSS_{train} ratio values of the six functional group, with percentage of presence in the study area.

Functional Group	% of cells with presence	AUC	TSS_{test}/ TSS_{train} ratio
Family Keratoisididae	43.21	0.642	0.890
Unbranched Keratoisididae	14.61	0.892	0.207
Branched 2D Keratoisididae	13.17	0.732	0.478
Branched 3D Keratoisididae	39.09	0.663	0.789
Branched 3D Keratoisididae (no *Acanella*)	20.37	0.882	0.231
Genus *Acanella*	29.01	0.706	0.971

3.3 Importance of environmental variables within each model

Jackknife tests of variable importance revealed the six models generated relied heavily on temperature and bathymetric variables, either BBPI/FBPI, slope or depth (Fig. 12). The only exceptions are represented by the models for the morphology branched 3D, where rugosity was the second major contributor when all genera were included, and salinity was the most important variable for the model when *Acanella* species were excluded.

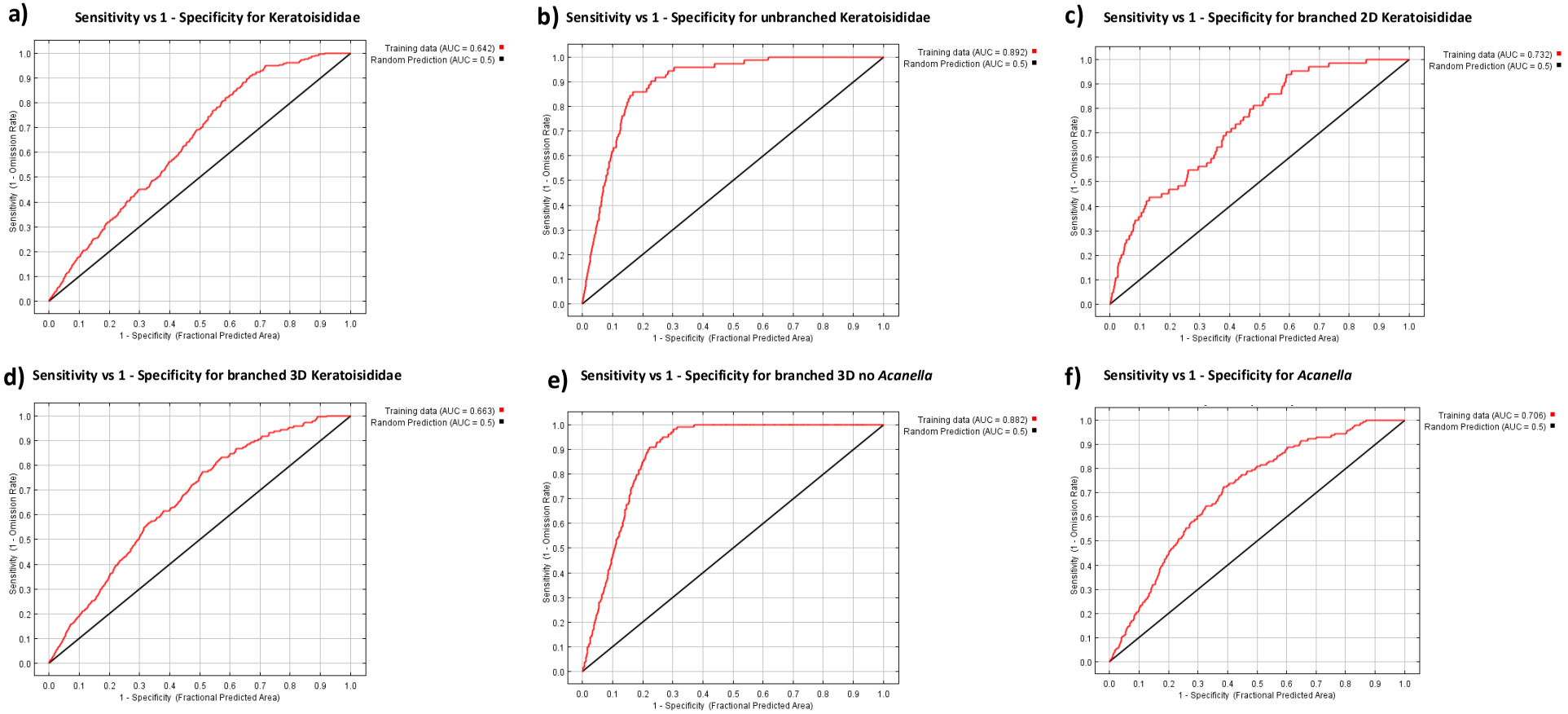

Figure 11. Receiver operating characteristic (ROC) curve for the six functional groups: (a) Keratoisididae, (b) unbranched Keratoisididae, (c) branched 2D Keratoisididae, (d) branched 3D Keratoisididae, (e) branched 3D Keratoisididae without *Acanella*, (f) *Acanella*.
The "Training data" (red line) shows the 'fit' of the model to the training data, while the "Random Prediction" (black line) is the ROC curve corresponding to random chance (Philips, 2017). Sensitivity is the proportion of predictions correctly predicted, while Specificity is the proportion of absences correctly predicted.

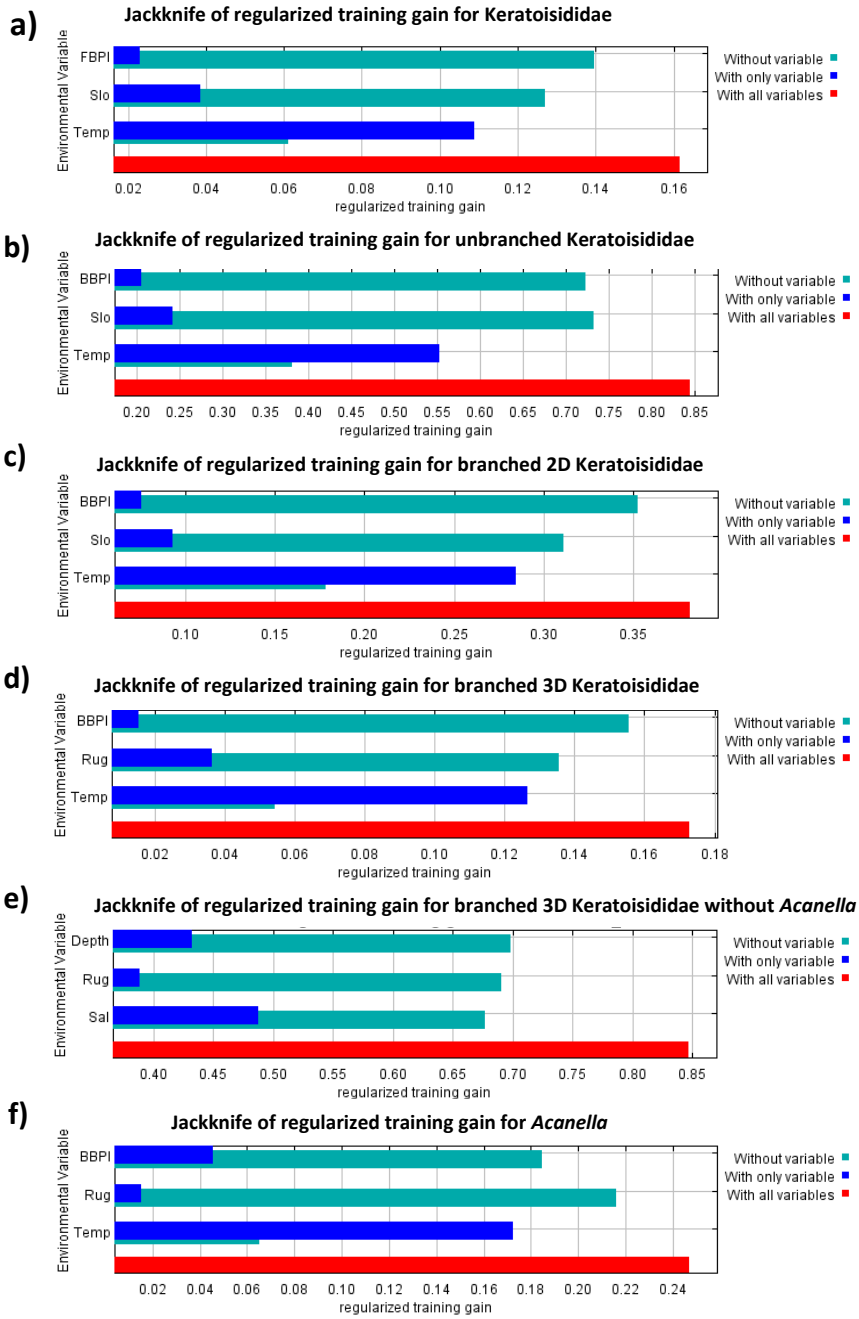

Figure 12. Jackknife of regularized training gain for (a) family Keratoisididae, (b) unbranched Keratoisididae, (c) branched 2D Keratoisididae, (d) branched 3D Keratoisididae, (e) branched 3D Keratoisididae without *Acanella*, (f) *Acanella*. The variables on the y-axis are those pre-selected with multi-model selection method, broad and fine bathymetric position indices (BBPI and FBPI), slope (Slo), temperature (Temp), rugosity (Rug) and salinity (Sal).

"Without variable" – each variable is excluded in turn and a model created with the remaining variables; "With only variable" – model built using only one variable; "With all variables" – full model.

3.4 Predicted distributions

The predicted distributions derived with MaxEnt extended along the Irish continental shelf (Fig. 13, 14, 15).

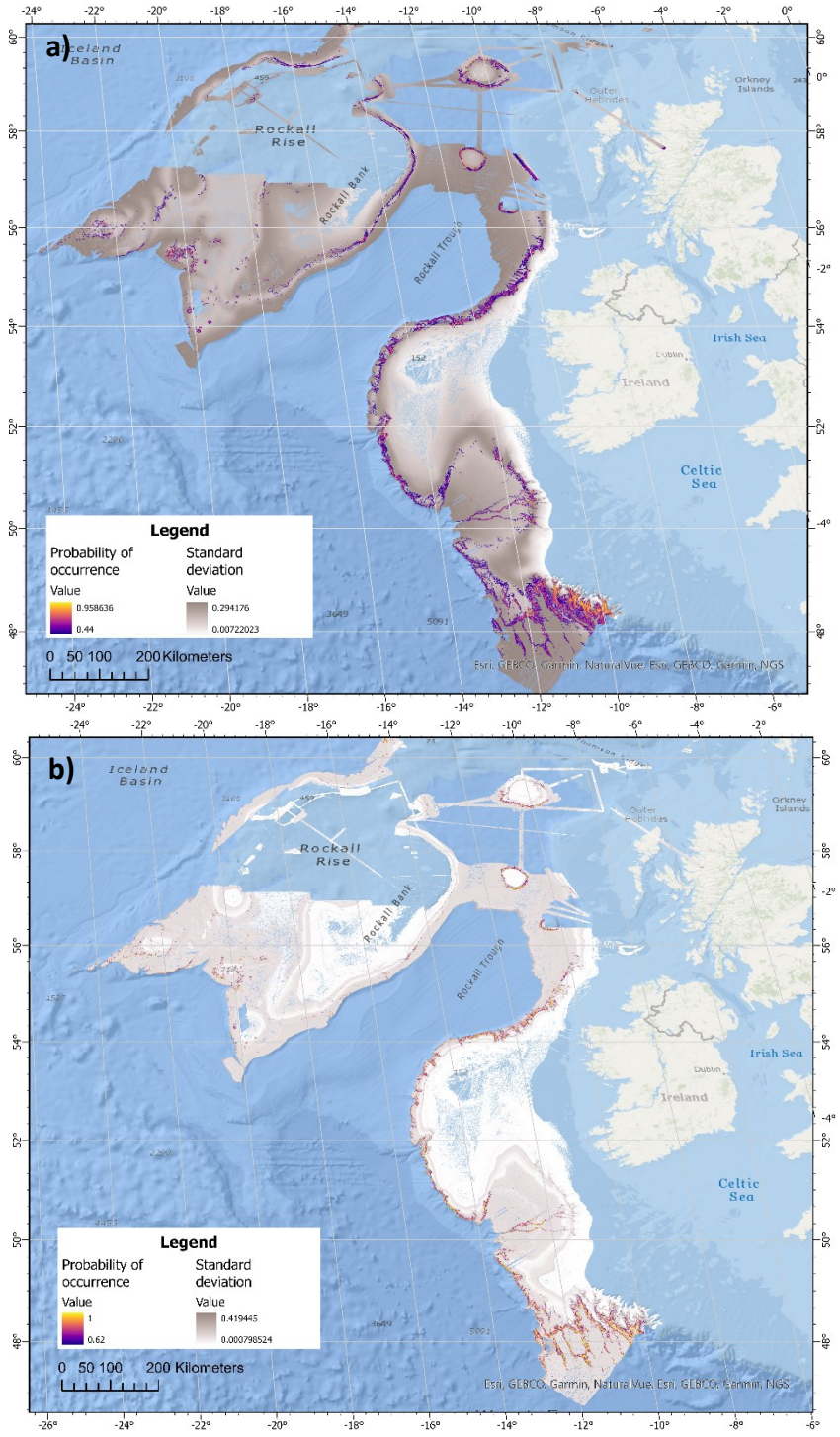

Figure 13. Distribution maps (probability of occurrence) of family Keratoisididae (a) and morphology unbranched (b). The probabilities showed in the maps go from the threshold value (purple) found for each group – see Table 4 for the values – to 1 (yellow). The standard deviation (grey layers) derives from the 10 training-test partitions.

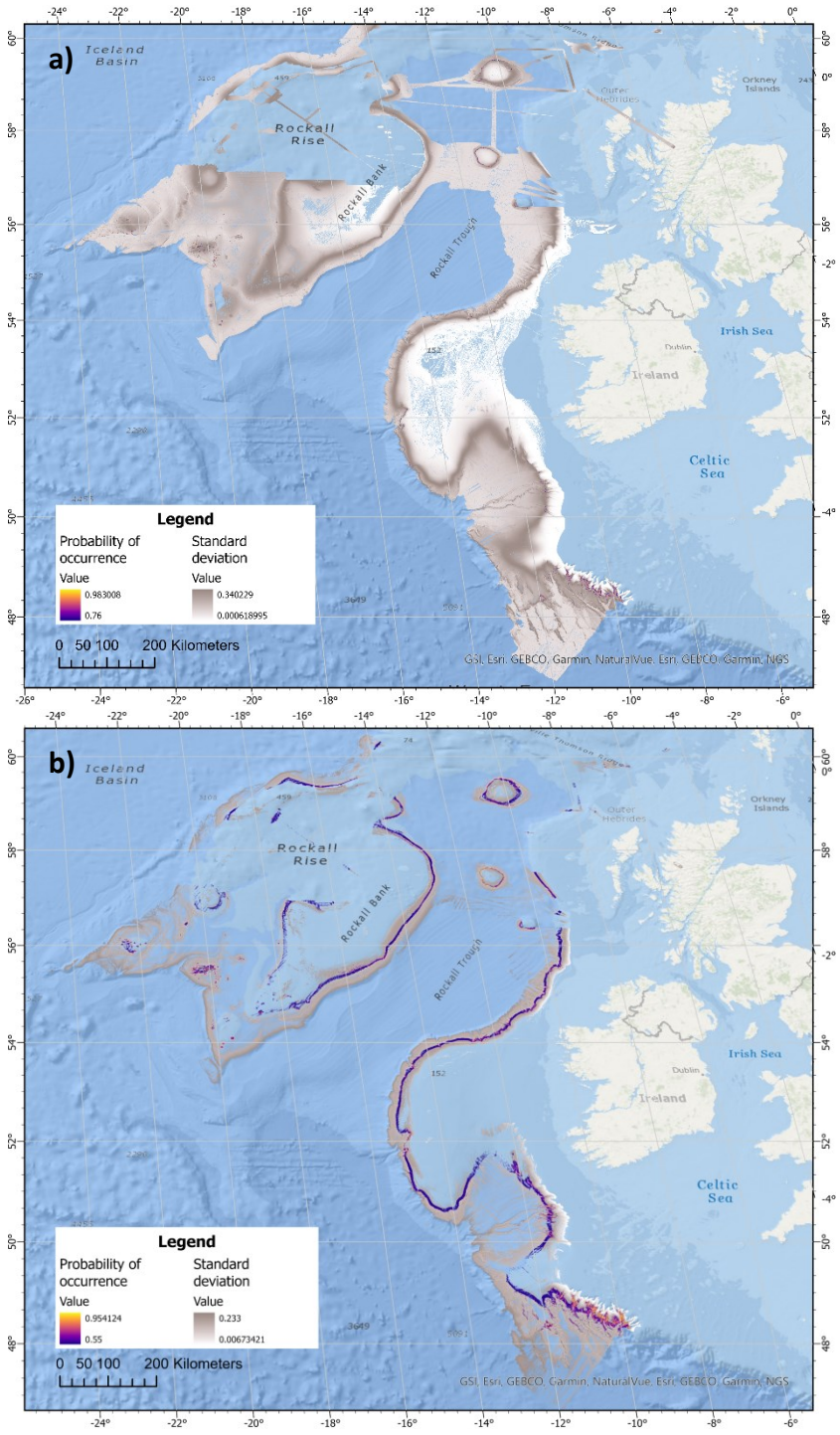

Figure 14. Distribution maps (probability of occurrence) of morphologies branched 2D (a) and branched 3D (b). The probabilities showed in the maps go from the threshold value (purple) found for each group – see Table 4 for the values – to 1 (yellow). The standard deviation (grey layers) derives from the 10 training-test partitions.

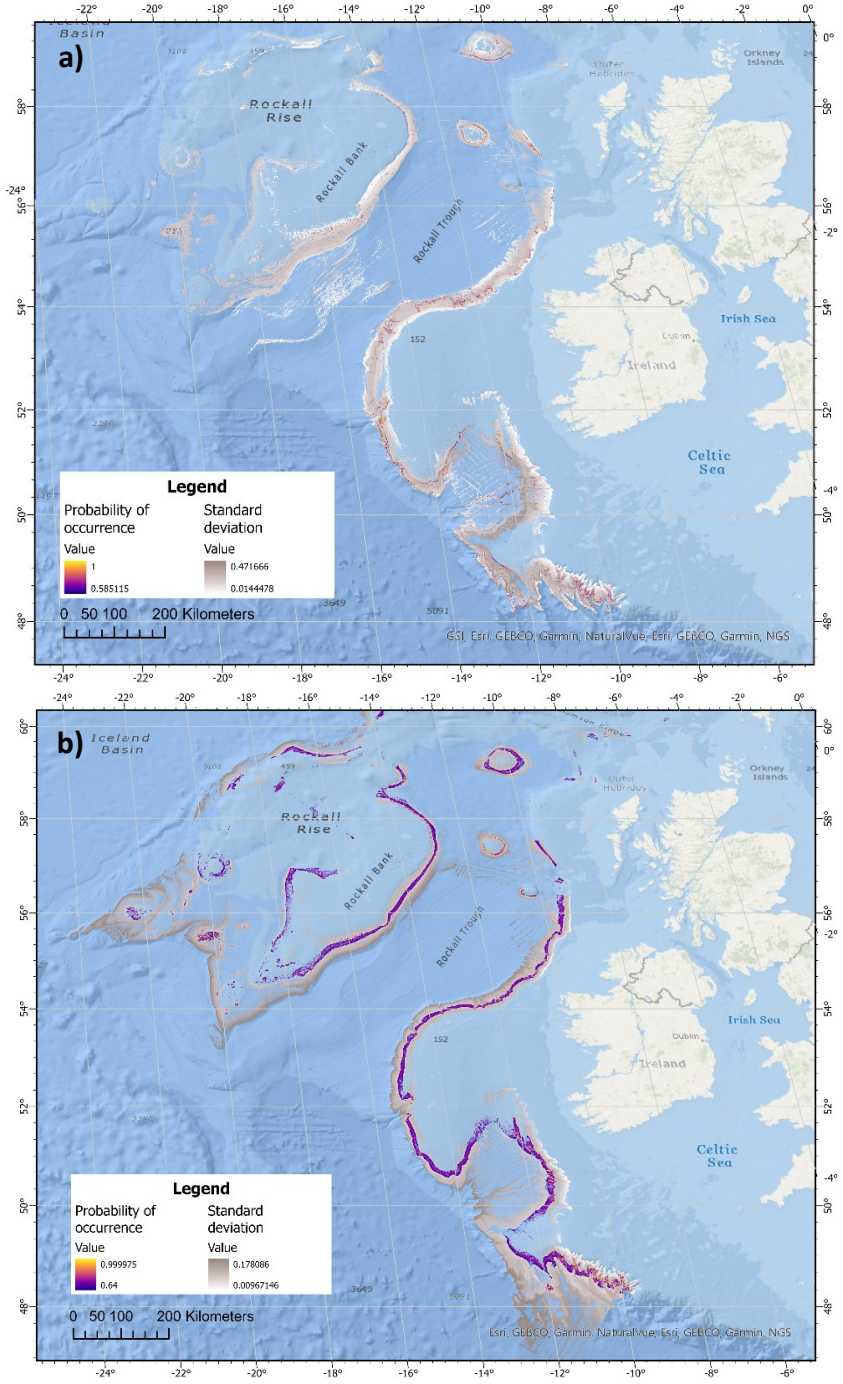

Figure 15. Distribution maps (probability of occurrence) of morphology branched 3D without *Acanella* (a) and genus *Acanella* (b). The probabilities showed in the maps go from the threshold value (purple) found for each group – see Table 4 for the values – to 1 (yellow). The standard deviation (grey layers) derives from the 10 training-test partitions.

Overall, the probabilities of occurrence were higher in the Whittard Canyon area and were more or less spread on the margin of Porcupine and Rockall banks, and on the sides of Anton Dohrn Seamount. The entire family Keratoisididae, as expected, had a widespread predicted distribution, but a high probability of occurrence confined in determined areas, such as Whittard Canyon (Fig. 13a).

The map for unbranched bamboo corals showed a high probability to find this morphology near vertical walls, such as along canyons and on the edge of the continental shelf, while branched 2D were the least spread, with only a hotspot of presences in the area preceding Whittard canyon (Fig. 13b, 14a). Instead, branched 3D Keratoisididae demonstrated a greater covered area, specifically in zones right before vertical walls, with also some occurrences in Fangorn Bank (Fig. 14b). Excluding the *Acanella* species from this morphology, the distribution changed, showing a high probability of occurrence in the Whittard canyon area, but also in the Gollum channel system (Fig. 15a). The map for the *Acanella* was very similar to that for the bush/arbuscular morphology (Fig. 15b), underlining the different preferences of habitat of this genus compared to the other bush Keratoisididae.

3.5 Ecological species niche comparison

From the boxplots of the distribution by the singular variables selected for the models (BBPI, rugosity, salinity, slope and temperature), it emerged that the three morphologies of Keratoisididae and the genus *Acanella* were found within the same ranges of temperature, slope and rugosity (Fig. 16).

Regardless of their morphology, Keratoisididae were mainly observed at 5-6°C, and within a moderately positive slope degree range (10-20°), and an even narrower range of rugosity (1.02-1.07). As for the distribution by salinity, the boxplots showed a difference in the width based on the morphology of Keratoisididae: unbranched and branched 3D tolerated a wider range of salinity, while the range for branched 2D and branched 3D without *Acanella* is narrower (Fig. 17a). However, the mean values of salinity are almost the same, between 35.4 and 35.5. For the BBPI values a difference between branched 3D and the other morphologies was found (Fig. 17b). Unbranched and branched 2D Keratoisididae showed a preference for positive BBPI values, which represent cliff edges or ridges. Branched 3D bamboo corals, both with and without *Acanella*, were distributed within a negative range of BBPI, that is linked to depressions or valley bottoms. The mean value close to 0 for the genus *Acanella* indicated the preference of these corals for plains.

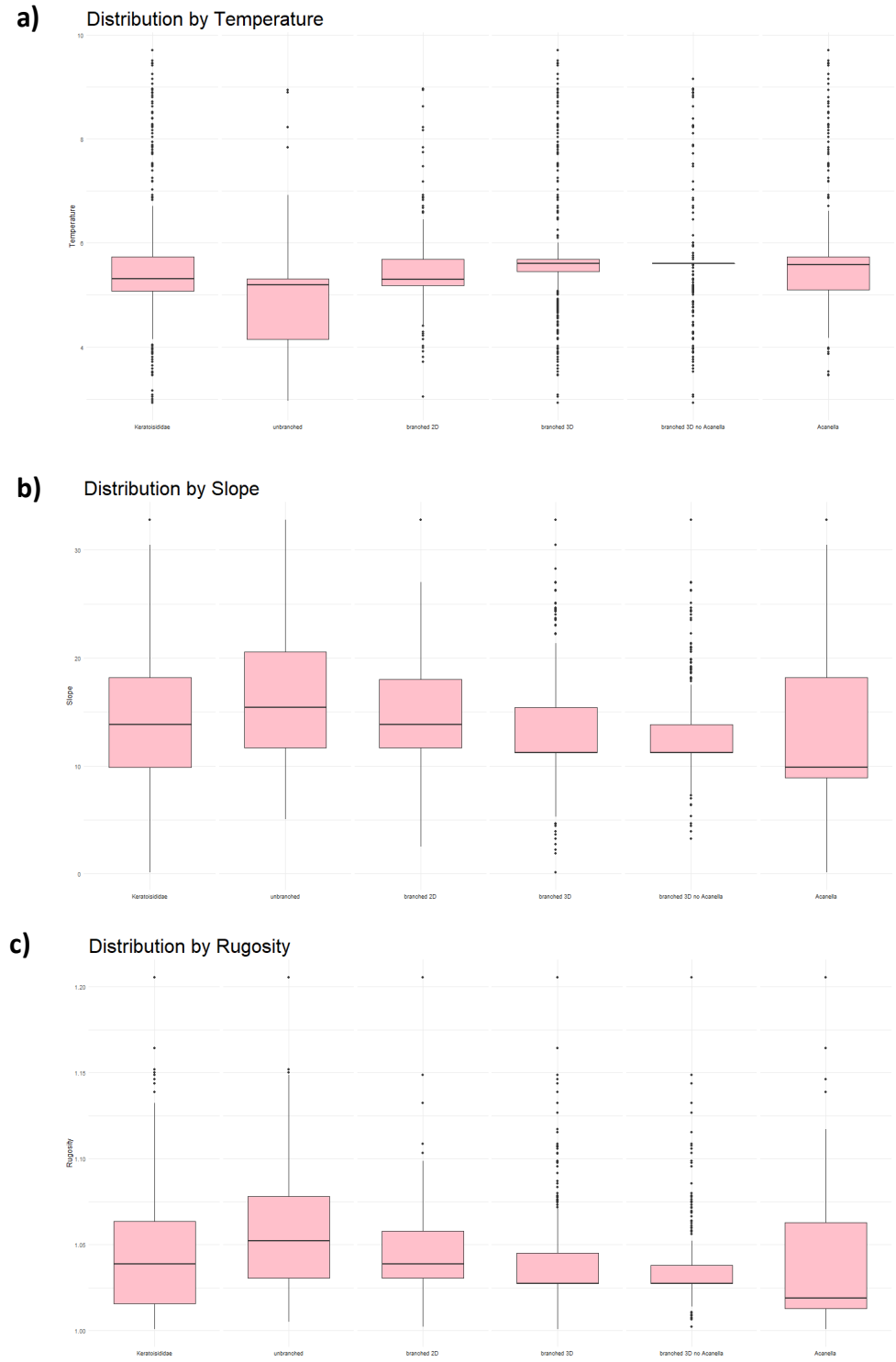

Figure 16. Distribution of the six functional group by temperature (a), slope (b) and rugosity (c).

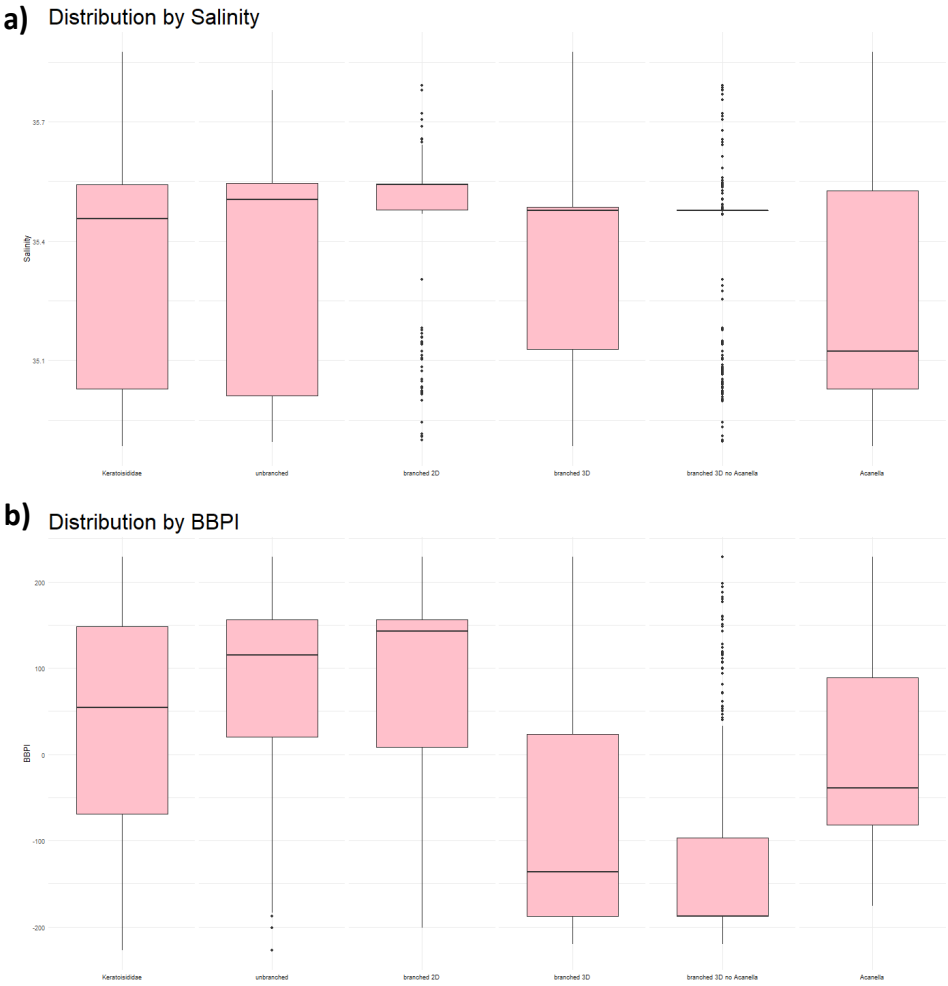

Figure 17. Distribution of the six functional group by salinity (a) and BBPI (b).

The results of Kruskal-Wallis test highlighted significant differences between the distributions of the three morphologies for all the considered environmental variables (Tab. 8). Dunn's test for *post hoc* pairwise comparisons pointed out that the ranges of temperature within which the four functional groups distribute were significantly different (p-values < 0.05) (Tab. 8a); for salinity, only branched 3D and unbranched morphologies were not significantly different (Tab. 8d); distributions by slope, rugosity and BBPI were significantly different between the morphologies and the genus *Acanella*, with the exception of branched 2D and unbranched bamboo corals, for which a p-value greater than 0.05 was calculated (Tab. 8b, c, e).

Table 8 (In this page and continued in the next). Results of Kruskal-Wallis test and Dunn's test for the comparisons of the distribution of the functional groups by the different environmental variables: (A) temperature, (B) slope, (C) rugosity, (D) salinity, (E) broad bathymetric position index (BBPI).

For each pair of functional groups, it is reported first the p-value obtained with the Kruskal-Wallis test, and then the Bonferroni-corrected p-values from the Dunn's test. Differences in the distributions by the different environmental variables are significant if p-values < 0.05 (chosen

Kruskal-Wallis rank sum test

data: Temperature by Functional group

Kruskal-Wallis chi-squared = 566.36, df = 3, p-value < $2.2 \cdot 10^{-16}$

(A)	Unbranched	Branched 2D	Branched 3D no *Acanella*	*Acanella*
Unbranched	-	0.000	0.000	0.000
Branched 2D	0.000	-	0.000	0.000
Branched 3D no *Acanella*	0.000	0.000	-	0.002
Acanella	0.000	0.000	0.002	-

Kruskal-Wallis rank sum test

data: Slope by Functional group

Kruskal-Wallis chi-squared = 481.63, df = 3, p-value < $2.2 \cdot 10^{-16}$

(B)	Unbranched	Branched 2D	Branched 3D no *Acanella*	*Acanella*
Unbranched	-	1.000	0.000	0.000
Branched 2D	1.000	-	0.000	0.000
Branched 3D no *Acanella*	0.000	0.000	-	0.000
Acanella	0.000	0.000	0.000	-

Kruskal-Wallis rank sum test

data: Rugosity by Functional group

Kruskal-Wallis chi-squared = 507.76, df = 3, p-value < $2.2 \cdot 10^{-16}$

(C)	Unbranched	Branched 2D	Branched 3D no *Acanella*	*Acanella*
Unbranched	-	1.000	0.000	0.000
Branched 2D	1.000	-	0.000	0.000
Branched 3D no *Acanella*	0.000	0.000	-	0.000
Acanella	0.000	0.000	0.000	-

Table 8. (continued) Results of Kruskal-Wallis test and Dunn's test.

Kruskal-Wallis rank sum test
data: Salinity by Functional group
Kruskal-Wallis chi-squared =500.21, df = 3, p-value < $2.2 \cdot 10^{-16}$

(D)	**Unbranched**	**Branched 2D**	**Branched 3D no *Acanella***	***Acanella***
Unbranched	-	0.000	0.402	0.000
Branched 2D	0.000	-	0.000	0.000
Branched 3D no *Acanella*	0.402	0.000	-	0.000
Acanella	0.000	0.000	0.000	-

Kruskal-Wallis rank sum test
data: BBPI by Group
Kruskal-Wallis chi-squared = 2299.5, df = 3, p-value < $2.2 \cdot 10^{-16}$

(E)	**Unbranched**	**Branched 2D**	**Branched 3D no *Acanella***	***Acanella***
Unbranched	-	0.128	0.000	0.000
Branched 2D	0.128	-	0.000	0.000
Branched 3D no *Acanella*	0.000	0.000	-	0.000
Acanella	0.000	0.000	0.000	-

4 DISCUSSION

In this thesis, predictive models were built for the coral family Keratoisididae, distinguishing between three main colony morphologies (unbranched, branched 2D and branched 3D) to verify the influence of this aspect on coral distribution.

4.1 *Keratoisididae distribution within the Irish Continental Margin*

Bamboo corals showed a widespread distribution within the study area, with high probability of occurrence along the edge of the continental shelf, along canyons, and on seamounts flanks (Fig. 13a). This result is supported by data reported in previous studies, which consolidated the presence of keratoisidids on the channels of the Whittard canyon system, and on the Anton Dohrn seamount (Amaro *et al.*, 2016; Morris *et al.*, 2013; Morrissey *et al.*, 2023b, 2022; Robert *et al.*, 2015). The high presence of corals on canyons and seamounts predicted in these models highlights how areas close to vertical walls in the deep-sea are important biodiversity hotspots. (Bostock *et al.*, 2015; Robert *et al.*, 2015).

Differences in the distributions of the morphology classes were observed, both in terms of extension and of location of hotspot areas. Models for unbranched Keratoisididae indicated a high probability of occurrence in the canyons and channels Morrissey *et al.* (2023) described along the shelf edge of Porcupine Bank, in the Gollum channel system and Whittard canyon system, and also on the flanks of the Anton Dohrn and Rosmary Bank seamounts (Fig. 13b). Branched bamboo corals seemed to have a less extensive distribution, and are confined to areas preceding vertical walls. The models for branched 2D bamboo corals highlighted presences at the head of the branches of the Whittard Canyon, near the edge of the continental shelf, in some sparse cell grids of the map in Porcupine Bank and Fangorn Bank, and on the seamounts (Fig. 14a). For the 3D morphology (without *Acanella* genus) the models predicted a scattered presence of individuals in Whittard Canyon, in an area even closer to the continental shelf, but probability of occurrence was found also on the sides of Anton Dohrn and Rosemary Bank seamounts, in the branches of Gollum channel system, and in areas dominated by coral mounds in Porcupine Bank, Porcupine Seabight and Rockall Bank (Fig. 15a) (Morrissey *et al.*, 2023b). Morris *et al.* (2013) observed the three morphologies of bamboo corals in different areas of Whittard Canyon, with whip corals extending more internally and deeper into the different ramifications of the canyon, while fan or bush shaped corals were observed closed to the continental shelf at shallower depths. This different location within canyons and channels could be linked to the different type of attachment to the substrate of the different morphologies. In general, bamboo corals have a holdfast that allows them to attach to rocky substrates such as those of vertical walls, but branching individuals

(both fan and bush shaped) often have a root-like system usually associated with mud substrates, such as those that characterize the upper slope of canyons, or with coral mounds (Altuna and Ríos, 2014; Amaro *et al.*, 2016; Baker *et al.*, 2012; Dueñas *et al.*, 2014; Saucier *et al.*, 2021). Further analyses are necessary to verify this distinction between the morphologies.

The results for the branched 3D morphology considered above were obtained by excluding the annotations of *Acanella*, since this genus is known to have a widespread distribution (Robert *et al.*, 2015; Saucier *et al.*, 2017). The model that considered all bamboo corals with a bush shape indicated a much more widespread distribution, and always in areas preceding vertical walls (Fig. 14b). Looking at the probability of occurrence obtained for the *Acanella* spp. (Fig. 15b), it is evident that the described distribution was influenced by the annotations relating to this genus, which constituted a conspicuous portion of the branching 3D dataset (Tab. 3). The distinctive appearance of the *Acanella* colonies makes it easy to identify these individuals during video annotation, and for this reason they are among the corals with relatively more records in the literature (Hughes and Gage, 2004; Morris *et al.*, 2013; Morrissey *et al.*, 2022; Robert *et al.*, 2015; Saucier *et al.*, 2021; Sayago-Gil *et al.*, 2012). In addition, these bamboo corals are known to be broadcast spawners, which explains their predicted wide distribution on the maps and the high number of occurrences (Buhl-Mortensen *et al.*, 2015). The predicted occurrences on the continental shelf confirm the preference of *Acanella* spp. for soft sediments, where they can settle thanks to their root-like system (Altuna and Ríos, 2014; Morris *et al.*, 2013).

The high probabilities of occurrence at canyon level, especially near Whittard canyon, could be linked to fact that most of the ROV dives were carried out in that area. There is clearly a sampling bias, which was also highlighted by the results obtained in the evaluation of the models. The models with higher AUC scores were those based on fewer observations, and compared to much larger datasets, there is greater risk of incurring a potential geographical influence (Baker *et al.*, 2022; Elith and Franklin, 2013; ICES, 2021; Syfert *et al.*, 2013). Sampling locations close to each other, and in places with probably similar environmental conditions (i.e., canyons and channels), might have delineated the specific niches of the three morphologies, but actually the real niches occupied by the different corals were not explored in their entirety (Stolar and Nielsen, 2015). This is why, despite the good performance, the models built for these functional groups were more overfitted than the models that considered annotations of individuals more scattered within the study area. The low values of the TSS_{test}/TSS_{train} ratio indicated that these models lack validation, i.e. they lack generality and cannot be used outside the dataset considered (Allouche *et al.*, 2006; Parimbelli, 2023; Radosavljevic and Anderson, 2014).

From AUC scores and TSS_{test}/TSS_{train} ratios it is also evident that individuals within a coral family can occupy very different niches. For the entire family Keratoisididae the model output provided predictions not better than random, which however represented reality better. Indeed, corals belonging to this family were observed in various locations within the study area, characterized by different environmental conditions (Bostock *et al.*, 2015; Morris *et al.*, 2013; Morrissey *et al.*, 2023b, 2022). Instead, model evaluation for the genus *Acanella* showed a good performance and a great transferability, despite the large number of observations widely distributed within the Irish Margin. This highlights that a lower taxonomic level, such as a genus, includes specimens that occupy the same ecological niche, and it is therefore preferable when building species distribution models.

4.2 Environmental parameters influencing morphologies distributions

The models presented in this thesis were built after selecting the most influential combination of environmental parameters, which turned out to be very similar among the six groups of bamboo corals considered. With the exception of branched 3D without *Acanella* morphology, temperature and BBPI (FBPI in the case of the family Keratoisididae) were selected for all functional groups; slope, rugosity and salinity were the other variables chosen as important in the various combinations. This finding is not so surprising, because other studies have already identified these parameters as those that mostly restrict deep-sea octocorals distribution (Dullo *et al.*, 2008; Edinger *et al.*, 2011; Howell *et al.*, 2011; Lapointe *et al.*, 2020; Yesson *et al.*, 2012). Temperature is the factor generally thought to most limit the presence of bamboo corals, and this was confirmed by the results of Jackknife tests, which identified temperature as the variable with highest gain for the models (Baker *et al.*, 2012; Fabri *et al.*, 2017; Roberts, 2009). The only exception was represented by branched 3D morphology without *Acanella* spp., for which it was found that the model was based more on salinity information, and indeed, looking at the distributions by salinity, this group was characterized by a narrower tolerance range than the others (Fig. 12d). However, comparison tests highlighted equal distributions by salinity for branched 3D and unbranched morphologies (p-values > 0.05), and significant differences for other functional groups.

The influence of such variables on the predictive models indicates that the distribution of bamboo corals is largely driven by bathymetry, since the thermohaline properties of water depend on the structure of water masses (Castro *et al.*, 1998). Depending on the depth considered, waters with different origins flow, and they are characterized by specific temperature and salinity ranges. In the specific case of the NE Atlantic Margin, upper layers (100-600 m) are

dominated by the Eastern North Atlantic Central Water (ENACW), characterized by a range of temperature from 12 to 4.3°C; in the intermediate waters, which extend down to 1200-1300 m, maximum salinity of the order of 36 is found, associated with a relatively high temperature (7-10°C), that corresponds to the flow of Mediterranean Outflow Water (MOW); below, at great depths (< 1500), the Labrador Sea Water mass marks the salinity minimum (~34.96), and together with the underlying North Atlantic Deep Water (NADW) it constitutes the deep waters with a considerably homogeneous temperature from 4.3 to 1°C (Castro *et al.*, 1998; Howell *et al.*, 2010; Morris *et al.*, 2013; Morrissey *et al.*, 2023b). The depths at which the ROV dives were conducted, and therefore corals used in this study were observed, fall within the vertical extent where the ENACW and the MOW flow. this could explain the distribution of the six functional groups within similar temperature and salinity ranges shown by the boxplots (Fig. 12a, d). Despite the similarities of the ranges at a visual level, statistical comparison tests indicated the presence of significant differences. Kruskal-Wallis test and *post hoc* Dunn's test highlighted differences in the temperature range of distributions within which the three morphologies are distributed, since the p-values of all pairwise comparisons were < 0.05. Indeed, from previous studies, it emerged that genera associated with a branched 3D morphology are mostly found in different temperature ranges from those found for typically unbranched genera (Bostock *et al.*, 2015; Brooke *et al.*, 2017).

In general, unbranched bamboo corals would be expected to occupy a specific ecological niche, different from that occupied by the other morphologies. Branching Keratoisididae are characterized by an increased surface area, which may suggest similar needs in terms of hydrodynamics and geomorphological conditions. During surveys conducted in the NE Atlantic, whip keratoisidids were generally found at greater depths, on the flanks of seamounts and of canyons, but also on the muddy bottoms of the latter (Morris *et al.*, 2013; Morrissey *et al.*, 2022). Branched morphologies, instead were mainly observed on gentle slopes (Baker *et al.*, 2012; Morrissey *et al.*, 2022).

From the results presented in this thesis it emerged that unbranched and branched 2D morphologies grow in similar locations characterized by the same terrain. Pairwise comparison tests highlighted that, for the available dataset, these functional groups share the preference for the same slope, roughness and BBPI values. From the boxplots for rugosity and slope it is not possible to determine how the distribution of the two shapes differ from that of branched 3D, because the ranges shown are very similar to each other. Instead, the plots for BBPI highlighted a clear difference. Specifically, unbranched and branched 2D keratoisidids were observed in benthic zones characterized by very positive bathymetric position indices, generally associated with upper slopes, cliff edge and ridges (Fig. 18) (Lucatelli *et al.*, 2020; Wright *et al.*, 2006). Bush bamboo corals, on the contrary, seemed to prefer places characterized by negative BBPI values,

which are associated with depressions, valley bottoms and cliff bases. This finding confirms the presence of unbranched and branched 2D morphologies on upper slopes, close to vertical walls, that was predicted by the models, but it contradicts the probability of occurrence of branched 3D morphology in continental shelf areas preceding canyons and vertical walls. Nevertheless, these ranges for BBPI values make sense when the relationship between slope and hydrodynamic movements is considered. Geomorphology of seabed reflects hydrodynamic conditions (Howell *et al.*, 2011; Ross *et al.*, 2015). Considering the Irish continental shelf, the upper slopes are dominated by either moderate or strong tidal currents, while at greater depths in the canyons and deep-sea channels, these currents are very weak (Amaro *et al.*, 2016; Morrissey *et al.*, 2023b). It is therefore expected that massive coral colonies developed three-dimensionally grow preferentially in valleys and depressions below vertical walls, as they are likely not to tolerate high velocity currents which can cause breakage. On the other hand, whip-like structures adapt better to these conditions. A single branch can also move freely following the current, increasing in this way the possibility of capturing particles and thus nutrient uptake.

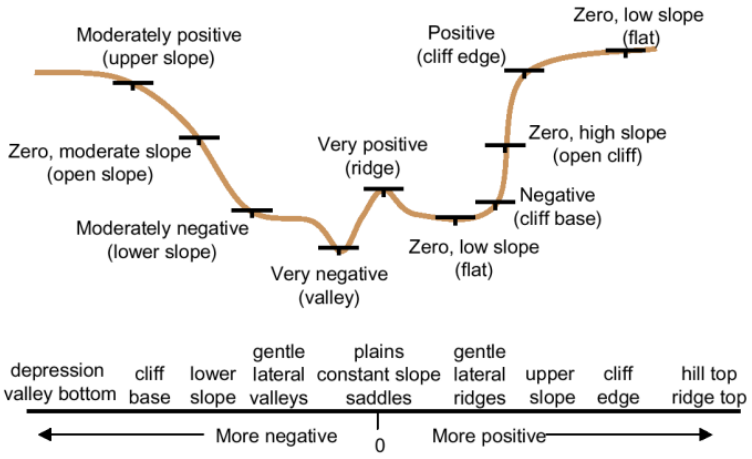

Figure 18. Correspondence between BBPI values and terrain geomorphology. The figure is based on topographic position index by Weiss (2001). Image taken from Weiss (2001).

In addition, by comparing the ranges within which the functional groups were distributed, it was further confirmed that the genus *Acanella* is distinct from the other branched 3D bamboo corals. Pairwise comparison tests highlighted significant differences for all the variables considered, which in the boxplots were visible above all for salinity and BBPI. *Acanella* spp. showed a wider range of tolerance for salinity compared to that of branched 3D morphology, which can be explained by the varied span of areas such individuals can occupy (Robert *et al.*, 2016). The distribution of annotations of this genus around values close to 0 for BBPI underlined the preference of these specimens for flat seabed, such as plains or saddles (Wright *et al.*, 2006).

It is necessary to take into account that multiple comparison procedures, as the Kruskal-Wallis and Dunn tests applied in this study, increase the possibility of a Type I error (false positive), i.e. rejecting a null hypothesis when the null hypothesis is true (Sato, 1996). The Bonferroni correction is most used to adjust multiple comparisons, due to its simplicity. It reduces the p-value dividing it by the number of comparisons, keeping the chance of making a Type I error at 5%. In this way it is possible to prevent false positive results, but caution is necessary in relying only on p-values in making decisions, because this method could be too conservative and inappropriately strict (Barnett *et al.*, 2022; Rice *et al.*, 2008).

4.3 Limitations of the study

Species distribution models have been widely used to predict the distribution of deep-sea species (Downie *et al.*, 2021; Reiss *et al.*, 2011; Sundahl *et al.*, 2020; Yesson *et al.*, 2012), however there are still limitations to the approach, mainly related to sampling bias, bathymetric data resolution, lack of knowledge for the species studied, and difficulties in marine imaging.

High costs and logistical difficulties due to the lack of equipment to collect high-quality samples extremely limit the possibility of deep-sea surveys (Barbosa *et al.*, 2020; Howell *et al.*, 2021). This leads to a limitation of the available data on which to carry out research, and generally the collection of thess data is concentrated in certain areas (e.g., Whittard canyon in the case of this study), often close to each other. This is in contrast to the assumption of no bias in presence locations adopted when modelling species distributions in MaxEnt using presence-only data (Araújo and Guisan, 2006). Failure to meet this assumption can result in a bias in the environmental spaces in which probability of occurrence are modelled, i.e. in a possible sampling bias (Baker *et al.*, 2022; Stolar and Nielsen, 2015). As previously mentioned, sampling bias, together with small sample size, can lead to an inaccurate identification of suitable areas (Elith and Franklin, 2013; ICES, 2021; Syfert *et al.*, 2013). Although these consequences on model performance have been demonstrated, so far only a few studies have attempted to address the problem (Araújo and Guisan, 2006; Bystriakova *et al.*, 2012; Kramer-Schadt *et al.*, 2013; Stolar and Nielsen, 2015; Syfert *et al.*, 2013). The probability of incurring a sampling bias could be reduced by using regularly spaced data collection and at a higher resolution, so that there is a complete observation of environmental conditions (Barbosa *et al.*, 2020; Dolan *et al.*, 2008; Howell *et al.*, 2022; Shelmerdine and Shucksmith, 2015). This could make the identification of niches occupied by species more accurate.

The probability of occurrence reported in this thesis are based exclusively on the environmental data used to build models. This means that a different resolution

of the data considered, and a different combination of parameters that influence the distribution of keratoisidids could lead to different results. For example, in this study the composition of the substrate and the speed of the currents were not considered, and these two factors are those that probably most influence the distribution of bamboo corals (Baker *et al.*, 2012; Howell *et al.*, 2011; Lapointe *et al.*, 2020; Morris *et al.*, 2013). Data regarding the composition of substrates is either collected from backscatter, but such information is not always available for the full extent of the study, or it is manually annotated during ROV video observation (Bennecke and Metaxas, 2017; Howell *et al.*, 2011). However, depending on the authors and the aim of the study, various categories of substrate can be identified, and so data from various cruise's surveys in different years are often non-homogeneous and not comparable. For the currents, data for the study area are available in the ICES (International Council for the Exploration of the Sea) archive and were collected during hydrological cruises (van Aken, 2000). However, the ArcGIS layers of this parameter available for the Irish continental slope did not extend to the Fangorn Bank sampling location, so it was not possible to consider the influence of this factor on keratoisidids distribution for the dataset used.

Other limitations come with marine images. Change of field of view, missed observations, misidentification of species, misspelling and subsequent taxonomic revisions represent problems related to video annotation. To minimize the impact of such possible errors, the studies should focus on family level (Etnoyer and Morgan, 2005). However, when modelling species distributions, this taxonomic level may not be the best to consider, because within families there can be individuals that occupy very different ecological niches. The predicted occurrences of these models are therefore no better than random predictions, as was found for the family Keratoisididae in this study. The model for the genus *Acanella* highlighted that a taxonomic level would be preferable in this type of study because it lumps together individuals that share the preference for similar environmental conditions. For bamboo corals, however, it is not possible to consider a lower taxonomic level, because the taxonomy of this group has been under constant revision. The continuous revision of keratoisidids genera is due to the extreme environments in which these corals are found, which makes it difficult to collect samples for genetic analysis; furthermore, the phenotypic plasticity within this group impedes finding characters useful for taxonomic identification (Dueñas and Sánchez, 2009; McFadden *et al.*, 2022; Morrissey *et al.*, 2022; Watling *et al.*, 2022). To determine whether morphology is a factor that influences the distribution of corals, it would be preferable to choose a coral family that includes easily distinguishable genera.

5 CONCLUSIONS

To improve the accuracy of species distribution models to be used for management policies, it is necessary to make sure to input environmental data that influence the distribution of the species considered. For deep-sea species, not all these parameters are known yet: the difficulties encountered in carrying out studies in such extreme environments do not allow an in-depth study of the ecology and biology of these species.

The aim of this thesis was to verify whether morphology is a factor that influences the distribution of deep-sea corals. The results show that, on the Irish Continental Margin, unbranched and 2D branching Keratoisididae colonies showed similar preferences in environmental conditions, while 3D branching colonies occupied a completely different ecological niche. It was confirmed that the genus *Acanella* prefers to grow on open plains, differently from the other branched 3D keratoisidids that tend to prefer gently slopes or depressions. In addition, the probabilities of distribution found with MaxEnt, when projected within the study area, highlighted a different distribution pattern for each of the functional groups considered.

An issue with this study was the use of a dataset with a strong environmental bias. Like many other studies conducted on deep-sea species, the concentration of resources in certain areas and the interest in investigating particular habitats meant that the sampling locations were concentrated in the same region of the Irish margin, and very close to each other. This, combined with the low number of annotations, could have identified specific ecological niches for the target species, when in reality all the possible environmental conditions for them have not been explored.

The results of this project provide a better understating of how bamboo corals are distributed in the NE Atlantic. Although the hypothesis that colony morphology influences the coral distribution was not fully accepted, these results highlighted the need of investigating the question further, perhaps with corals that show a reduced morphological plasticity.

APPENDIX A

Table 1. Code and Group transect values attributed to each event of each cruise's surveys from 2013 to 2021.

Code transect	Group transect	Year	Event
1	1	2013	7
2	2	2013	14
3	101	2013	15
4	101	2013	26
5	101	2013	27
6	6	2013	32
7	7	2013	36
8	8	2013	39
9	9	2013	44
9	9	2013	45
11	11	2013	52
12	108	2013	62
13	107	2013	76
14	14	2013	85
15	15	2013	89
16	16	2013	91
17	17	2014	5
18	105	2014	7
19	105	2014	9
21	109	2014	12
22	110	2014	17
23	110	2014	25
24	24	2014	27
24	24	2014	76
26	105	2014	29
27	105	2014	30
28	110	2014	31
29	29	2014	33
30	112	2016	2
31	112	2016	3
32	32	2016	5
33	33	2016	10
34	108	2016	21
35	108	2016	22
36	109	2016	27
37	109	2016	30
38	106	2016	32
39	106	2016	33
40	107	2016	37
41	110	2016	59
42	110	2016	60
43	43	2016	62
44	44	2016	65
45	104	2016	79
48	105	2016	84
49	49	2016	87
50	103	2016	89
51	103	2016	91
52	102	2016	93
53	53	2017	2
54	54	2017	3
55	55	2017	5
56	56	2017	6
57	57	2017	8
58	58	2017	9
59	59	2017	13
60	102	2017	15
61	102	2017	16
62	104	2017	18
63	104	2017	19
64	104	2017	20
65	104	2017	21
66	104	2017	23
67	104	2017	24
68	104	2017	25
69	112	2017	28
70	112	2017	29
71	111	2017	30
72	111	2017	31
73	73	2018	5
74	101	2018	7
75	101	2018	8
76	76	2018	9
77	77	2018	14
78	78	2018	15
79	100	2018	16
80	100	2018	17
81	81	2018	18
82	82	2018	19
83	83	2018	20
84	84	2018	21
85	85	2018	22
86	86	2018	23
87	87	2018	24
200	113	2021	PG1
201	201	2021	1
202	113	2021	2
203	203	2021	3
204	204	2021	4
205	205	2021	5
207	207	2021	7
209	209	2021	9
210	210	2021	10
211	211	2021	11
212	212	2021	12
213	213	2021	13

APPENDIX B

Highlights of genera, species and morphological clades present in the local species identification guide. The taxonomy is based on the classification given by Morrissey *et al.* (2022); the genera previously attributed to the morphotypes are also reported. The images are stills taken by ROV *Holland I* during the expeditions conducted from 2013 to 2021.


Acanella arbuscula
Yellowish/orange/light pink – Light and delicate in appearance, with a main branch bamboo like and more or less dense branching.


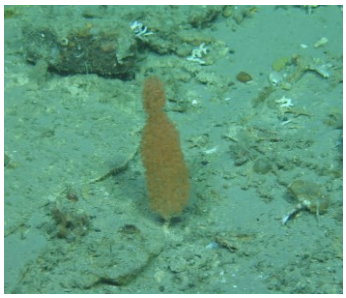

***Acanella* indet spp.**
Yellowish/orange/light pink – Bushy with dense polyps, with a main branch bamboo like.

***Isidella* indet spp.**
Light orange to light pink – Many branches, more or less in a 2D plan with a candelabrum-like shape.


Keratoisididae Clade B1 m1

Pink/white – Few branches with zig-zag shape; polyps are quite long and spaced with each other.

Previously *Lepidisis* morphotype.


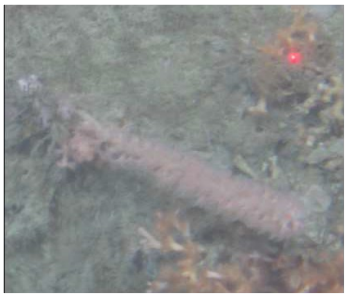

Keratoisididae Clade B1 m2

Light orange to light pink – Unbranched, quite straight and thick with the polyps.

Previously *Keratoisis* morphotype.


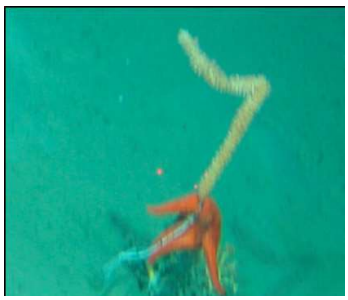

Keratoisididae Clade B1 m3

Pink/white – Unbranched, with zig-zag whip shape; polyps are quite long and spaced with each other

Previously *Keratoisis* morphotype.


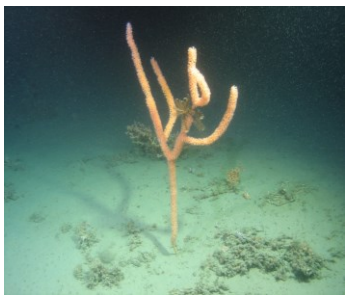

Keratoisididae Clade B1 m4

Light orange to light pink – Few branches, quite thick with the polyps.

Previously *Keratoisis* morphotype.

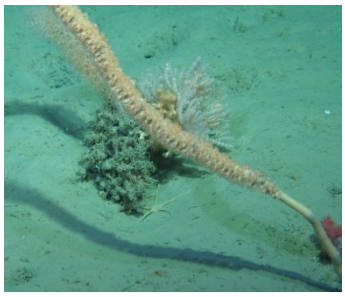
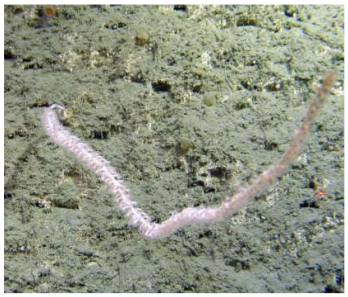

Keratoisididae Clade C1 m1

Light orange to light pink, polyps with red mouth – Unbranched, not a straight branch but not curled either; quite thick with the polyps.

Previously *Lepidisis* morphotype.


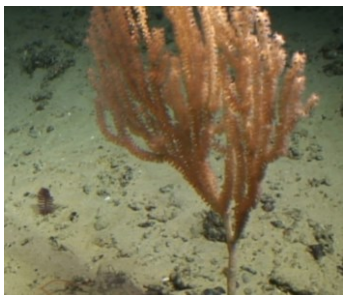

Keratoisididae Clade D1 m1

Pink – Overall V shape, with branches rising vertically from a small segment of naked skeleton; fat polyps close to each other.


Keratoisididae Clade D2 m1

Light orange to light pink – Few branches, quite thick with the polyps.

Previously *Keratoisis* morphotype.

Keratoisididae Clade F1 m1

Light pink – Unbranched and slender; polyps long and quite spaced with each other.

Previously *Lepidisis* morphotype.


Keratoisididae Clade I1 m1

Pink – Many branches pointed towards all directions; it can be covered by yellow zoanthids.

Keratoisididae Clade I1 m2

Pale – Multiple branches emerging from a central hub at the base, similar to the previous clade but bigger; densely packed polyps. Likely *Eknomisis* indet spp.


Keratoisididae Clade I1 m3

Pale – Multiple branches emerging from a central hub at the base; densely packed polyps.


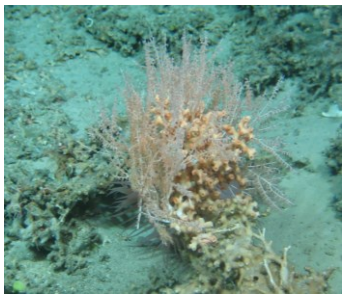

Keratoisididae Clade I1 m4

Pale – Bushy from the base, with thin and quite dense branches.

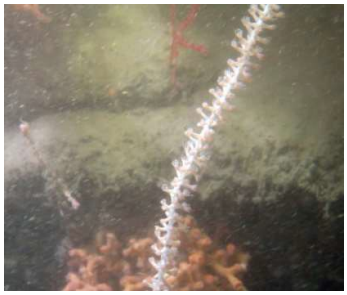

Keratoisididae Clade I1 m5

Light pink – Unbranched; long polyps quite spaced with each other.
Previously *Lepidisis* morphotype.


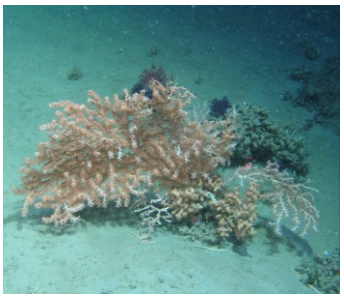

Keratoisididae Clade J3 m1

Light orange to light pink – Many branches, more or less in a 2D plan.
Previously *Jasonisi* morphotype.


Keratoisididae Clade J3 m2

Light orange to light pink – Many branches, more or less in a 2D plan; polyps look more delicate than m1.
Previously *Keratoisis* morphotype.

APPENDIX C

Table 1. Features deselected and regularization parameters chosen to train the final models for the six functional groups considered, with the corrected Akaike information criterion (AICc) of the resultant model.

Functional group	Feature		Regularization parameter	
	Feature deselected	AICc	Value	AICc
Family Keratoisididae	no auto, no hinge, no threshold	2551.337	0.011	2549.107
Unbranched morphology	no auto, no hinge	817.477	0.187	-9366.319
Branched 2D morphology	no hinge, no threshold	762.048	0.002	756.387
Branched 3D morphology	no auto, no hinge, no threshold	2305.506	0.099	2296.959
Branched 3D morphology without *Acanella* spp.	no auto, no hinge	1187.503	0.112	-18584.841
Genus *Acanella*	no auto, no hinge, no threshold	1681.206	0.5	1680.017

Table 2. Corrected Akaike information criterion (AICc) of the pre-selected combination of environmental variables for each of the six functional groups.

Functional group	Combination of variables	AICc value
Family Keratoisididae	FBPI – Slo – Temp	543.443
Unbranched morphology	BBPI – Slo – Temp	322.469
Branched 2D morphology	BBPI – Slo – Temp	332.639
Branched 3D morphology	BBPI – Rug – Temp	540.386
Branched 3D morphology without Acanella spp.	Depth – Rug – Sal	429.7486
Genus Acanella	BBPI – Rug – Temp	491.466

APPENDIX D

Figure 1. QQ-plots for BBPI across the different functional group.

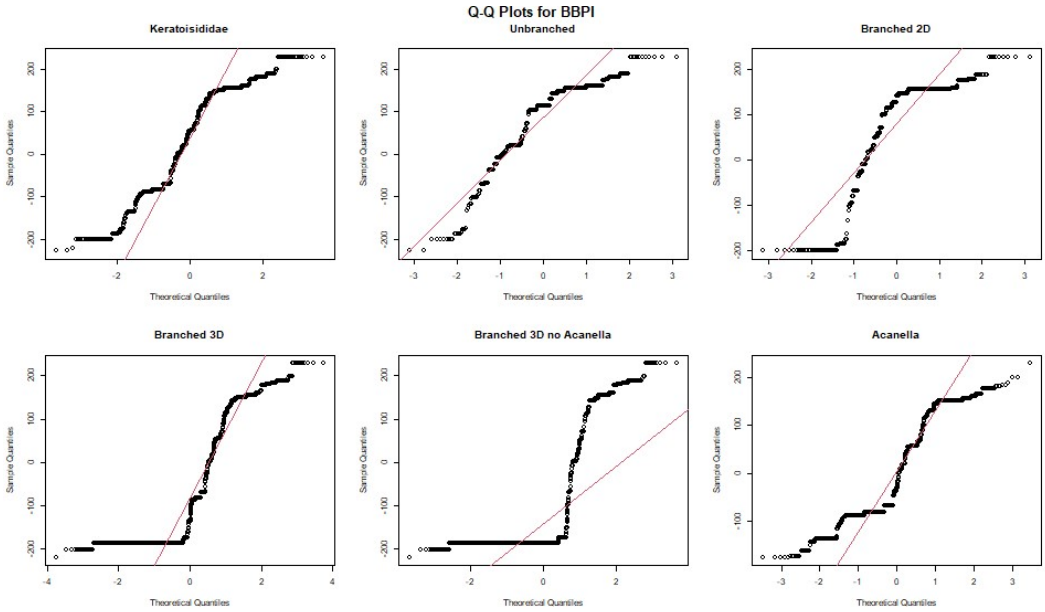

Figure 2. QQ-plots for Rugosity across the different functional group.

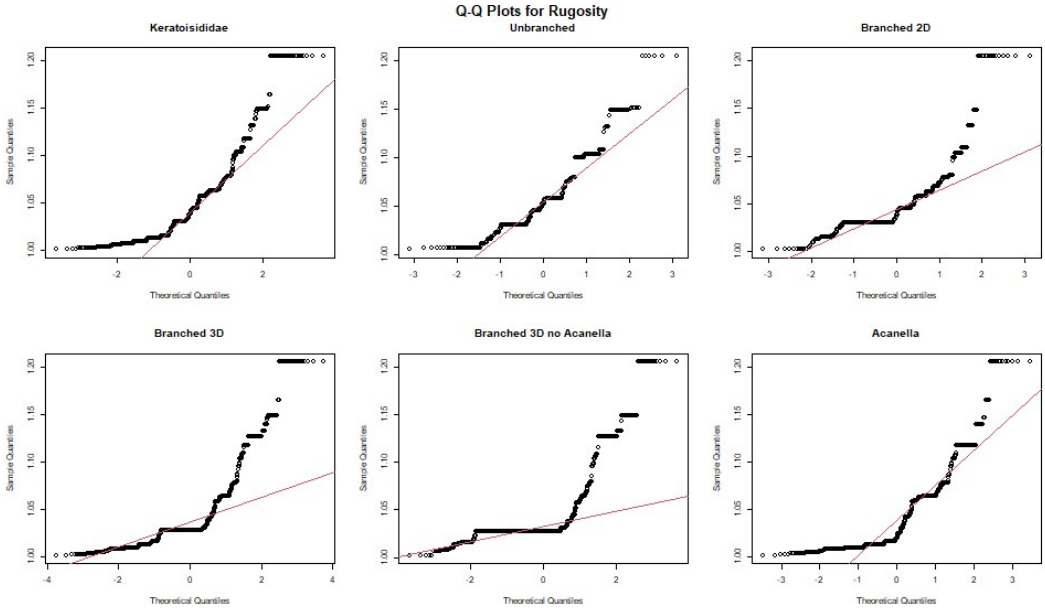

Figure 3. QQ-plots for Salinity across the different functional group.

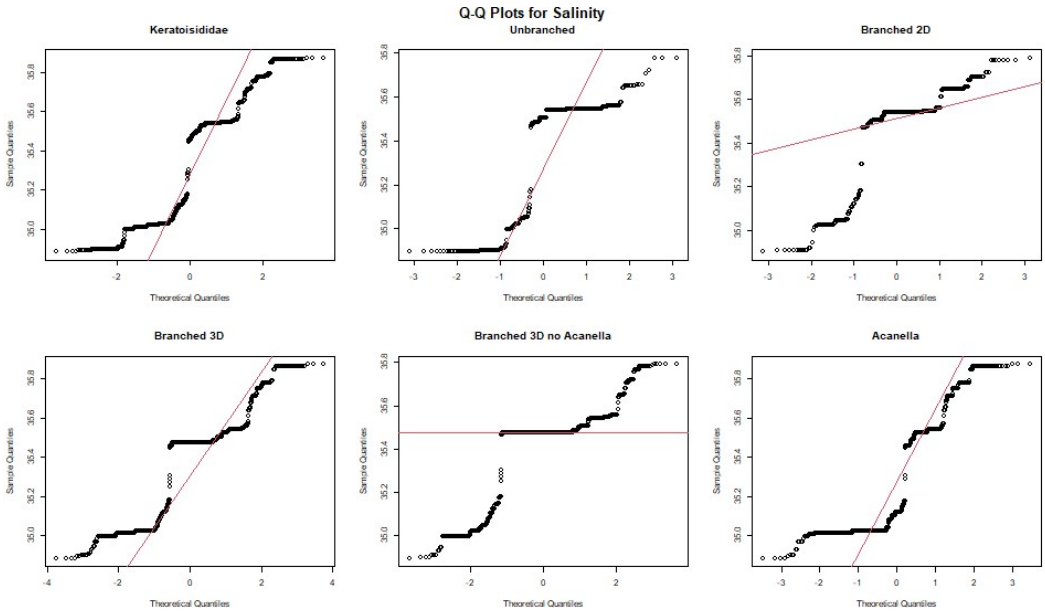

Figure 4. QQ-plots for Slope across the different functional group.

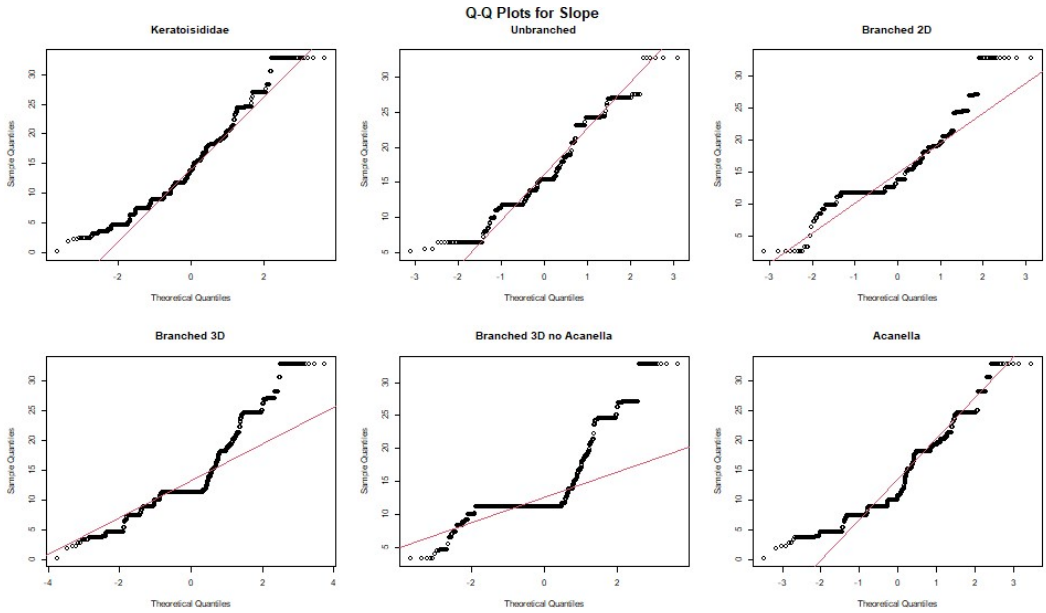

Figure 5. QQ-plots for Temperature across the different functional group.

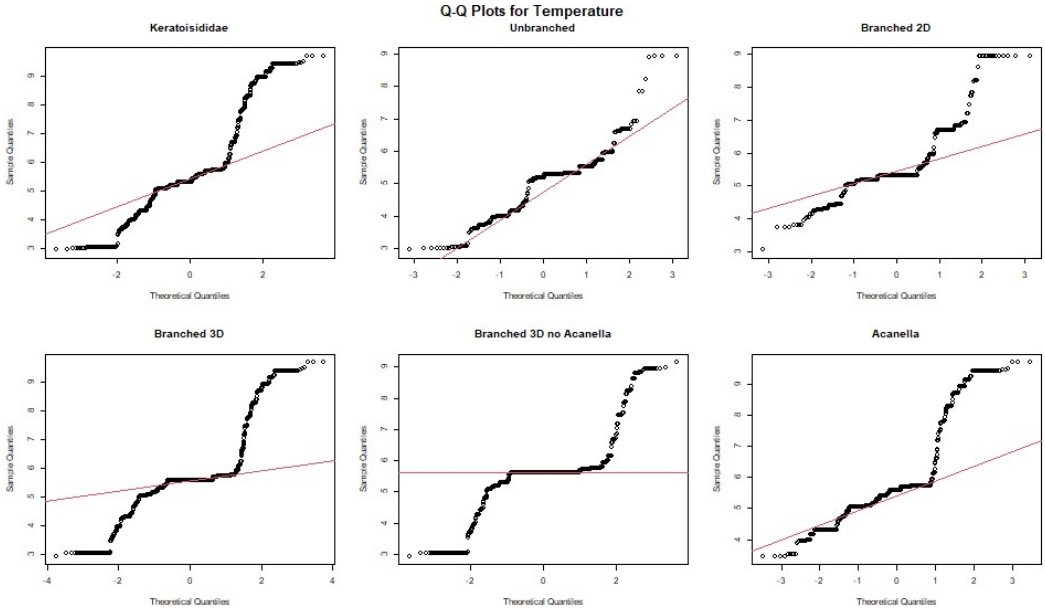

BIBLIOGRAPHY

Allouche, O., Tsoar, A., Kadmon, R., 2006. Assessing the accuracy of species distribution models: prevalence, kappa and the true skill statistic (TSS): Assessing the accuracy of distribution models. Journal of Applied Ecology 43, 1223–1232. https://doi.org/10.1111/j.1365-2664.2006.01214.x

Altuna, Á., Ríos, P., 2014. Calcaxonian octocorals (Cnidaria: Anthozoa) from DEMERSALES, ECOMARG and INDEMARES expeditions to bathyal waters off north and northwest Spain (northeast Atlantic). *XVIII Iberian Symposium of Marine Biology Studies*, Gijò, Spain.

Amaro, T., Huvenne, V.A.I., Allcock, A.L., Aslam, T., Davies, J.S., Danovaro, R., De Stigter, H.C., Duineveld, G.C.A., Gambi, C., Gooday, A.J., Gunton, L.M., Hall, R., Howell, K.L., Ingels, J., Kiriakoulakis, K., Kershaw, C.E., Lavaleye, M.S.S., Robert, K., Stewart, H., Van Rooij, D., White, M., Wilson, A.M., 2016. The Whittard Canyon – A case study of submarine canyon processes. Progress in Oceanography 146, 38–57. https://doi.org/10.1016/j.pocean.2016.06.003

Araújo, M.B., Anderson, R.P., Márcia Barbosa, A., Beale, C.M., Dormann, C.F., Early, R., Garcia, R.A., Guisan, A., Maiorano, L., Naimi, B., O'Hara, R.B., Zimmermann, N.E., Rahbek, C., 2019. Standards for distribution models in biodiversity assessments. Sci. Adv. 5, eaat4858. https://doi.org/10.1126/sciadv.aat4858

Araújo, M.B., Guisan, A., 2006. Five (or so) challenges for species distribution modelling. Journal of Biogeography 33, 1677–1688. https://doi.org/10.1111/j.1365-2699.2006.01584.x

Baker, D.J., Maclean, I.M.D., Goodall, M., Gaston, K.J., 2022. Correlations between spatial sampling biases and environmental niches affect species distribution models. Global Ecol. Biogeogr. 31, 1038–1050. https://doi.org/10.1111/geb.13491

Baker, K., Wareham, V., Snelgrove, P., Haedrich, R., Fifield, D., Edinger, E., Gilkinson, K., 2012. Distributional patterns of deep-sea coral assemblages in three submarine canyons off Newfoundland, Canada. Mar. Ecol. Prog. Ser. 445, 235–249. https://doi.org/10.3354/meps09448

Barbosa, R.V., Davies, A.J., Sumida, P.Y.G., 2020. Habitat suitability and environmental niche comparison of cold-water coral species along the Brazilian continental margin. Deep Sea Research Part I: Oceanographic Research Papers 155, 103147. https://doi.org/10.1016/j.dsr.2019.103147

Barnett, M.J., Doroudgar, Shadi., Khosraviani, Vista., Ip, E.J., 2022. Multiple comparisons: To compare or not to compare, that is the question. Research

in Social and Administrative Pharmacy 18, 2331–2334. https://doi.org/10.1016/j.sapharm.2021.07.006

Bennecke, S., Metaxas, A., 2017. Is substrate composition a suitable predictor for deep-water coral occurrence on fine scales? Deep Sea Research Part I: Oceanographic Research Papers 124, 55–65. https://doi.org/10.1016/j.dsr.2017.04.011

Bostock, H.C., Tracey, D.M., Currie, K.I., Dunbar, G.B., Handler, M.R., Mikaloff Fletcher, S.E., Smith, A.M., Williams, M.J.M., 2015. The carbonate mineralogy and distribution of habitat-forming deep-sea corals in the southwest pacific region. Deep Sea Research Part I: Oceanographic Research Papers 100, 88–104. https://doi.org/10.1016/j.dsr.2015.02.008

Bourque, J.R., Demopoulos, A.W.J., 2018. The influence of different deep-sea coral habitats on sediment macrofaunal community structure and function. PeerJ 6, e5276. https://doi.org/10.7717/peerj.5276

Brooke, S.D., Watts, M.W., Heil, A.D., Rhode, M., Mienis, F., Duineveld, G.C.A., Davies, A.J., Ross, S.W., 2017. Distributions and habitat associations of deep-water corals in Norfolk and Baltimore Canyons, Mid-Atlantic Bight, USA. Deep Sea Research Part II: Topical Studies in Oceanography 137, 131–147. https://doi.org/10.1016/j.dsr2.2016.05.008

Buhl-Mortensen, L., Mortensen, P.B., 2004. Symbiosis in Deep-Water Corals.

Buhl-Mortensen, L., Olafsdottir, S.H., Buhl-Mortensen, P., Burgos, J.M., Ragnarsson, S.A., 2015. Distribution of nine cold-water coral species (Scleractinia and Gorgonacea) in the cold temperate North Atlantic: effects of bathymetry and hydrography. Hydrobiologia 759, 39–61. https://doi.org/10.1007/s10750-014-2116-x

Burk, C.A., Drake, C.L. (Eds.) 2013. The Geology of Continental Margins. Springer.

Burnham, K.P., Anderson, D.R., 1998. Practical Use of the Information-Theoretic Approach, in: Burnham, K.P., Anderson, D.R. (Eds.), Model Selection and Inference: A Practical Information-Theoretic Approach. Springer, New York, NY, pp. 75–117. https://doi.org/10.1007/978-1-4757-2917-7_3

Burnham, K.P., Anderson, D.R., Huyvaert, K.P., 2011. AIC model selection and multimodel inference in behavioral ecology: some background, observations, and comparisons. Behav Ecol Sociobiol 65, 23–35. https://doi.org/10.1007/s00265-010-1029-6

Bystriakova, N., Peregrym, M., Erkens, R.H.J., Bezsmertna, O., Schneider, H., 2012. Sampling bias in geographic and environmental space and its effect on the predictive power of species distribution models. Systematics and Biodiversity 10, 305–315. https://doi.org/10.1080/14772000.2012.705357

Cairns, S.D., 2007. Deep-water corals: an overview with special reference to diversity and distribution of deep-water scleractinian corals. Bulletin of Marine Science 81.

Castro, C.G., Pérez, F.F., Holley, S.E., Ríos, A.F., 1998. Chemical characterisation and modelling of water masses in the Northeast Atlantic. Progress in Oceanography 41, 249–279. https://doi.org/10.1016/S0079-6611(98)00021-4

Conti, L.A., Lim, A., Wheeler, A.J., 2019. High resolution mapping of a cold water coral mound. Sci Rep 9, 1016. https://doi.org/10.1038/s41598-018-37725-x

Convention on Biological Diversity, 2008. COP 9 Decision IX/20. Marine and coastal biodiversity [WWW Document]. URL https://www.cbd.int/decision/cop/?id=11663 Accessed on 11-2-23.

Danovaro, R., Corinaldesi, C., Dell'Anno, A., Snelgrove, P.V.R., 2017. The deep-sea under global change. Current Biology 27, R461–R465. https://doi.org/10.1016/j.cub.2017.02.046

Dinno, A., 2017. Package 'dunn.test'. CRAN Repos 10, 1–7.

Dinno, A., 2015. Nonparametric Pairwise Multiple Comparisons in Independent Groups using Dunn's Test. The Stata Journal 15, 292–300. https://doi.org/10.1177/1536867X1501500117

Dolan, M.F.J., Grehan, A.J., Guinan, J.C., Brown, C., 2008. Modelling the local distribution of cold-water corals in relation to bathymetric variables: Adding spatial context to deep-sea video data. Deep Sea Research Part I: Oceanographic Research Papers 55, 1564–1579. https://doi.org/10.1016/j.dsr.2008.06.010

Downie, A., Noble-James, T., Chaverra, A., Howell, K., 2021. Predicting sea pen (Pennatulacea) distribution on the UK continental shelf: evidence of range modification by benthic trawling. Mar. Ecol. Prog. Ser. 670, 75–91. https://doi.org/10.3354/meps13744

Dueñas, L., Sánchez, J., 2009. Character lability in deep-sea bamboo corals (Octocorallia, Isididae, Keratoisidinae). Mar. Ecol. Prog. Ser. 397, 11–23. https://doi.org/10.3354/meps08307

Dueñas, L.F., Alderslade, P., Sánchez, J.A., 2014. Molecular systematics of the deep-sea bamboo corals (Octocorallia: Isididae: Keratoisidinae) from New Zealand with descriptions of two new species of Keratoisis. Molecular Phylogenetics and Evolution 74, 15–28. https://doi.org/10.1016/j.ympev.2014.01.031

Dullo W, C., Flögel, S., Rüggeberg, A., 2008. Cold-water coral growth in relation to the hydrography of the Celtic and Nordic European continental margin. Mar. Ecol. Prog. Ser. 371, 165–176. https://doi.org/10.3354/meps07623

Dunn, O.J., 1964. Multiple Comparisons Using Rank Sums. American Statistical Association and American Society for Quality 6, 241–252.

Edinger, E.N., Sherwood, O.A., Piper, D.J.W., Wareham, V.E., Baker, K.D., Gilkinson, K.D., Scott, D.B., 2011. Geological features supporting deep-sea coral habitat in Atlantic Canada. Continental Shelf Research 31, S69–S84. https://doi.org/10.1016/j.csr.2010.07.004

Elith, J., Franklin, J., 2013. Species Distribution Modeling, in: Encyclopedia of Biodiversity. Elsevier, pp. 692–705. https://doi.org/10.1016/B978-0-12-384719-5.00318-X

Elith, J., H. Graham, C., P. Anderson, R., Dudík, M., Ferrier, S., Guisan, A., J. Hijmans, R., Huettmann, F., R. Leathwick, J., Lehmann, A., Li, J., G. Lohmann, L., A. Loiselle, B., Manion, G., Moritz, C., Nakamura, M., Nakazawa, Y., McC. M. Overton, J., Townsend Peterson, A., J. Phillips, S., Richardson, K., Scachetti-Pereira, R., E. Schapire, R., Soberón, J., Williams, S., S. Wisz, M., E. Zimmermann, N., 2006. Novel methods improve prediction of species' distributions from occurrence data. Ecography 29, 129–151. https://doi.org/10.1111/j.2006.0906-7590.04596.x

Elith, J., Leathwick, J.R., 2009. Species Distribution Models: Ecological Explanation and Prediction Across Space and Time. Annu. Rev. Ecol. Evol. Syst. 40, 677–697. https://doi.org/10.1146/annurev.ecolsys.110308.120159

Elith, J., Phillips, S.J., Hastie, T., Dudík, M., Chee, Y.E., Yates, C.J., 2011. A statistical explanation of MaxEnt for ecologists: Statistical explanation of MaxEnt. Diversity and Distributions 17, 43–57. https://doi.org/10.1111/j.1472-4642.2010.00725.x

Encyclopædia Britannica. Image "Continental margin". https://www.britannica.com/science/continental-margin#/media/1/135007/147308. Accessed on 2023-11-10

Esri Inc. 2020. ArcGIS Pro (Version 2.8). Redlands, CA: Esri Inc

Etnoyer, P., Morgan, L.E., 2005. Habitat-forming deep-sea corals in the Northeast Pacific Ocean, in: Freiwald, A., Roberts, J.M. (Eds.), Cold-Water Corals and Ecosystems. Springer Berlin Heidelberg, Berlin, Heidelberg, pp. 331–343. https://doi.org/10.1007/3-540-27673-4_16

Fabri, M.-C., Bargain, A., Pairaud, I., Pedel, L., Taupier-Letage, I., 2017. Cold-water coral ecosystems in Cassidaigne Canyon: An assessment of their environmental living conditions. Deep Sea Research Part II: Topical Studies

in Oceanography 137, 436–453. https://doi.org/10.1016/j.dsr2.2016.06.006

FAO, 2009. International Guidelines for the Management of Deep-sea Fisheries in the High Seas / Directives internationales sur la gestion de la pêche profonde en haute mer / Directrices Internacionales para la Ordenación de las Pesquerías de Aguas Profundas en Alta Mar. Rome, p. 73.

Feng, J.-C., Liang, J., Cai, Y., Zhang, S., Xue, J., Yang, Z., 2022. Deep-sea organisms research oriented by deep-sea technologies development. Science Bulletin 67, 1802–1816. https://doi.org/10.1016/j.scib.2022.07.016

Freeman, E.A., Moisen, G., 2008. PresenceAbsence : An R package for presence absence analysis. J. Stat. Soft. 23 (11): 31 p. https://doi.org/10.18637/jss.v023.i11

Freiwald, A., Fossa, J.H., Grehan, A., Koslow, T., Roberts, J.M., 2004. Cold-water coral reefs: out of sight-no longer out of mind. UNEP-WCMC.

Goreau, T.F., Goreau, N.I., Goreau, T.J., 1979. Corals and Coral Reefs. Scientific America 241, 124–137.

Guinan, J., Grehan, A., Dolan, M., Brown, C., 2009. Quantifying relationships between video observations of cold-water coral cover and seafloor features in Rockall Trough, west of Ireland. Mar. Ecol. Prog. Ser. 375, 125–138. https://doi.org/10.3354/meps07739

Guisan, A., Zimmermann, N.E., 2000. Predictive habitat distribution models in ecology. Ecological Modelling 135, 147–186. https://doi.org/10.1016/S0304-3800(00)00354-9

Harris, P.T., Whiteway, T., 2011. Global distribution of large submarine canyons: Geomorphic differences between active and passive continental margins. Marine Geology 285, 69–86. https://doi.org/10.1016/j.margeo.2011.05.008

Hernández-Molina, F.J., Llave, E., Stow, D.A.V., 2008. Chapter 19 Continental Slope Contourites, in: Developments in Sedimentology. Elsevier, pp. 379–408. https://doi.org/10.1016/S0070-4571(08)10019-X

Herring, P., 2001. The Biology of the Deep Ocean, Biology of Habitats. OUP Oxford.

Hessler, R., Sanders, H., 1967. Faunal diversity in the deep-sea. Deep Sea Research and Oceanographic Abstracts 14, 65–78. https://doi.org/10.1016/0011-7471(67)90029-0

Howe, J.A., Stoker, M.S., Masson, D.G., Pudsey, C.J., Morris, P., Larter, R.D., Bulat, J., 2006. Seabed morphology and the bottom-current pathways around Rosemary Bank seamount, northern Rockall Trough, North Atlantic.

Marine and Petroleum Geology 23, 165–181. https://doi.org/10.1016/j.marpetgeo.2005.08.003

Howell, K., Bridges, A., Graves, K., Allcock, L., La Bianca, G., Ventura-Costa, C., Donaldson, S., Downie, A., Furey, T., McGrath, F., Ross, R., 2022. Performance of deep-sea habitat suitability models assessed using independent data, and implications for use in area-based management. Mar. Ecol. Prog. Ser. 695, 33–51. https://doi.org/10.3354/meps14098

Howell, K.L., Davies, J.S., Narayanaswamy, B.E., 2010. Identifying deep-sea megafaunal epibenthic assemblages for use in habitat mapping and marine protected area network design. J. Mar. Biol. Ass. 90, 33–68. https://doi.org/10.1017/S0025315409991299

Howell, K.L., Hilario, A., Allcock, A.L., Bailey, D., Baker, M., Clark, M.R., ..., & Xavier, J.R., 2021. A decade to study deep-sea life. Nature Ecology & Evolution 5.3, 265–267.

Howell, K.L., Holt, R., Endrino, I.P., Stewart, H., 2011. When the species is also a habitat: Comparing the predictively modelled distributions of Lophelia pertusa and the reef habitat it forms. Biological Conservation 144, 2656–2665. https://doi.org/10.1016/j.biocon.2011.07.025

Huetten, E., Greinert, J., 2008. Software controlled guidance, recording and post-processing of seafloor observations by ROV and other towed devices: The software package OFOP. Presented at the EGU General Assembly 2008, Geophysical Research Abstracts, Vienna, Austria.

Hughes, D.J., Gage, J.D., 2004. Benthic metazoan biomass, community structure and bioturbation at three contrasting deep-water sites on the northwest European continental margin. Progress in Oceanography 63, 29–55. https://doi.org/10.1016/j.pocean.2004.09.002

Hutchinson, G.E., 1957. Concluding remarks. Cold Spring Harbor symposia on quantitative biology 22, 415–427.

ICES, 2021. Workshop on the Use of Predictive Habitat Models in ICES Advice (WKPHM). https://doi.org/10.17895/ICES.PUB.8213

INFOMAR (Integrated Mapping For the Suistainable Development of Ireland's Marine Resource). 2022. Foras na Mara Marine Institute. Retrieved from https://www.marine.ie/Home/site-area/irelands-marineresource/real-map-ireland

Karlsson, C., 2019. MaxEnt_TSS_calculations: R code file to produce TSS and kappa results from MaxEnt output. MIT License.

Kim, Y.-J., Gu, C., 2004. Smoothing Spline Gaussian Regression: More Scalable Computation via Efficient Approximation. Journal of the Royal Statistical Society Series B: Statistical Methodology 66, 337–356. https://doi.org/10.1046/j.1369-7412.2003.05316.x

Kramer-Schadt, S., Niedbella, J., Pilgrim, J.D., Schroder, B., Lindenborn, J., Reinfelder, V., Stillfried, M., Heckman, I., Scharf, A.K., Augeri, D.M., Cheyne, S.M., Hearn, A.J., Ross, J., Macdonald, D.W., Mathai, J., Eaton, J., Marshall, A.J., Semiadi, G., Rustam, R., Bernard, H., Alfred, R., Samejima, H., Duckworth, J.W., Breitenmoser-Wuersten, C., Belant, J.L., Hofer, H., Wilting, A., 2013. The importance of correcting for sampling bias in MaxEnt species distribution models. Diversity and Distributions 19, 1366–1379. https://doi.org/10.1111/ddi.12096

Kruskal, W.H., Wallis, W.A., 1952. Use of Ranks in One-Criterion Variance Analysis. Journal of the American Statistical Association 47, 583–621.

Lapointe, A., Watling, L., 2015. Bamboo corals from the abyssal Pacific: *Bathygorgia*. Proceedings of the Biological Society of Washington 128, 125–136. https://doi.org/10.2988/0006-324X-128.2.125

Lapointe, A., Watling, L., Gontz, A.M., 2020. Deep-sea benthic megafaunal communities on the New England and Corner Rise Seamounts, Northwest Atlantic Ocean, in: Seafloor Geomorphology as Benthic Habitat. Elsevier, pp. 917–932. https://doi.org/10.1016/B978-0-12-814960-7.00057-9

Lapointe, A.E., Watling, L., France, S.C., Auster, P.J., 2020. Megabenthic assemblages in the lower bathyal (700–3000 m) on the New England and Corner Rise Seamounts, Northwest Atlantic. Deep Sea Research Part I: Oceanographic Research Papers 165, 103366. https://doi.org/10.1016/j.dsr.2020.103366

Levin, L.A., Dayton, P.K., 2009. Ecological theory and continental margins: where shallow meets deep. Trends in Ecology & Evolution 24, 606–617. https://doi.org/10.1016/j.tree.2009.04.012

Linley, T.D., Lavaleye, M., Maiorano, P., Bergman, M., Capezzuto, F., Cousins, N.J., D'Onghia, G., Duineveld, G., Shields, M.A., Sion, L., Tursi, A., Priede, I.G., 2017. Effects of cold-water corals on fish diversity and density (European continental margin: Arctic, NE Atlantic and Mediterranean Sea): Data from three baited lander systems. Deep Sea Research Part II: Topical Studies in Oceanography 145, 8–21. https://doi.org/10.1016/j.dsr2.2015.12.003

Liu, C., Berry, P.M., Dawson, T.P., Pearson, R.G., 2005. Selecting thresholds of occurrence in the prediction of species distributions. Ecography 28, 385–393. https://doi.org/10.1111/j.0906-7590.2005.03957.x

Lucatelli, D., Goes, E.R., Brown, C.J., Souza-Filho, J.F., Guedes-Silva, E., Araújo, T.C.M., 2020. Geodiversity as an indicator to benthic habitat distribution: an integrative approach in a tropical continental shelf. Geo-Mar Lett 40, 911–923. https://doi.org/10.1007/s00367-019-00614-x

Macreadie, P.I., McLean, D.L., Thomson, P.G., Partridge, J.C., Jones, D.O.B., Gates, A.R., Benfield, M.C., Collin, S.P., Booth, D.J., Smith, L.L., Techera, E., Skropeta, D., Horton, T., Pattiaratchi, C., Bond, T., Fowler, A.M., 2018. Eyes in the sea: Unlocking the mysteries of the ocean using industrial, remotely operated vehicles (ROVs). Science of The Total Environment 634, 1077–1091. https://doi.org/10.1016/j.scitotenv.2018.04.049

Marine Institute, 2022a. The Real Map of Ireland [Image]. Foras na Mara Marine Institute. URL https://www.marine.ie/site-area/irelands-marine-resource/real-map-ireland-0 (accessed 10.30.23).

Marine Institute, 2022b. Deepwater ROV | Marine Institute [Image]. URL https://www.marine.ie/site-area/infrastructure-facilities/research-vessels/deepwater-rov (accessed 9.24.23).

McFadden, C.S., Van Ofwegen, L.P., Quattrini, A.M., 2022. Revisionary systematics of Octocorallia (Cnidaria: Anthozoa) guided by phylogenomics. BSSB 1. https://doi.org/10.18061/bssb.v1i3.8735

McKight, P.E., Najab, J., 2010. Kruskal-Wallis Test, in: The Corsini Encyclopedia of Psychology. John Wiley & Sons, Ltd, pp. 1–1. https://doi.org/10.1002/9780470479216.corpsy0491

Merow, C., Smith, M.J., Silander, J.A., 2013. A practical guide to MaxEnt for modeling species' distributions: what it does, and why inputs and settings matter. Ecography 36, 1058–1069. https://doi.org/10.1111/j.1600-0587.2013.07872.x

Miller, J., 2010. Species Distribution Modeling: Species distribution modeling. Geography Compass 4, 490–509. https://doi.org/10.1111/j.1749-8198.2010.00351.x

Morris, K.J., Tyler, P.A., Masson, D.G., Huvenne, V.I.A., Rogers, A.D., 2013. Distribution of cold-water corals in the Whittard Canyon, NE Atlantic Ocean. Deep Sea Research Part II: Topical Studies in Oceanography 92, 136–144. https://doi.org/10.1016/j.dsr2.2013.03.036

Morrissey, D., Gordon, J.D., Saso, E., Bilewitch, J.P., Taylor, M.L., Hayes, V., McFadden, C.S., Quattrini, A.M., Allcock, A.L., 2023a. Bamboozled! Resolving deep evolutionary nodes within the phylogeny of bamboo corals (Octocorallia: Scleralcyonacea: Keratoisididae). Molecular Phylogenetics and Evolution 188, 107910. https://doi.org/10.1016/j.ympev.2023.107910

Morrissey, D., Lim, A., Howell, K.L., White, M., Wheeler, A.J., Allcock, A.L., 2023b. The North-east Atlantic Margin: A Review of the Geology, Geography, Oceanography, and Vulnerable Megabenthic Ecosystems of the Continental Slope of Ireland and the United Kingdom, in: Oceanography and Marine Biology. CRC Press, Boca Raton, pp. 219–291. https://doi.org/10.1201/9781003363873-6

Morrissey, D., Untiedt, C.B., Croke, K., Robinson, A., Turley, E., Allcock, A.L., 2022. The Biodiversity of Calcaxonian Octocorals from the Irish Continental Slope Inferred from Multilocus Mitochondrial Barcoding. Diversity 14, 576. https://doi.org/10.3390/d14070576

Mouton, M.W., 2013. The Continental Shelf. Springer.

Neves, B.D.M., Wareham Hayes, V., Herder, E., Hedges, K., Grant, C., Archambault, P., 2020. Cold-Water Soft Corals (Cnidaria: Nephtheidae) as Habitat for Juvenile Basket Stars (Echinodermata: Gorgonocephalidae). Front. Mar. Sci. 7, 547896. https://doi.org/10.3389/fmars.2020.547896

NOAA, n.d. What is the “deep” ocean? Ocean Exploration Facts: NOAA Office of Ocean Exploration and Research [WWW Document]. URL https://oceanexplorer.noaa.gov/facts/deep-ocean.html (accessed 10.29.23).

Parimbelli, A., 2023. Selecting the best framework to model Antipatharia distributions in the Northeast Atlantic deep sea. Not published yet.

Parimbelli, A., 2020. Invertebrate associations with deep-sea corals and sponges on the Irish Continental Margin (Laurea Magistrale). Università degli Studi di Padova.

Phillips, S.J., 2017. A Brief Tutorial on Maxent.

Phillips, S.J., 2009. Sample selection bias and presence-only distribution models: implications for background and pseudo-absence data. Ecological Applications 181–197.

Phillips, S.J., Anderson, R.P., Schapire, R.E., 2006. Maximum entropy modeling of species geographic distributions. Ecological Modelling 190, 231–259. https://doi.org/10.1016/j.ecolmodel.2005.03.026

Phillips, S.J., Dudík, M., 2008. Modeling of species distributions with Maxent: new extensions and a comprehensive evaluation. Ecography 31, 161–175. https://doi.org/10.1111/j.0906-7590.2008.5203.x

Phillips, S.J., Dudík, M., Schapire R.E. [Internet] Maxent software for modeling species niches and distributions (Version 3.4.1). Available from url:

http://biodiversityinformatics.amnh.org/open_source/maxent/. Accessed on 2023-11-10.

Pierrejean, M., Grant, C., Neves, B.D.M., Chaillou, G., Edinger, E., Blanchet, F.G., Maps, F., Nozais, C., Archambault, P., 2020. Influence of Deep-Water Corals and Sponge Gardens on Infaunal Community Composition and Ecosystem Functioning in the Eastern Canadian Arctic. Front. Mar. Sci. 7, 495. https://doi.org/10.3389/fmars.2020.00495

Pohlert, T., 2018. Package 'PMCMRplus'. CRAN Repos version 1.4.1.

R Core Team (2020). R: *A language and environment for statistical computing. R Foundation for Statistical Computing* (Version 4.4.4) [Computer Software]. Vienna, Austria. https://www.R-ptoject.org/

Radosavljevic, A., Anderson, R.P., 2014. Making better M AXENT models of species distributions: complexity, overfitting and evaluation. J. Biogeogr. 41, 629–643. https://doi.org/10.1111/jbi.12227

Ramirez-Llodra, E. (Ed.), 2020. Deep-Sea Ecosystems: Biodiversity and Anthropogenic Impacts, in: The Law of the Seabed. Brill | Nijhoff, pp. 36–60. https://doi.org/10.1163/9789004391567_004

Ramirez-Llodra, E., Brandt, A., Danovaro, R., De Mol, B., Escobar, E., German, C.R., Levin, L.A., Martinez Arbizu, P., Menot, L., Buhl-Mortensen, P., Narayanaswamy, B.E., Smith, C.R., Tittensor, D.P., Tyler, P.A., Vanreusel, A., Vecchione, M., 2010. Deep, diverse and definitely different: unique attributes of the world's largest ecosystem. Biogeosciences 7, 2851–2899. https://doi.org/10.5194/bg-7-2851-2010

Reiss, H., Cunze, S., König, K., Neumann, H., Kröncke, I., 2011. Species distribution modelling of marine benthos: a North Sea case study. Mar. Ecol. Prog. Ser. 442, 71–86. https://doi.org/10.3354/meps09391

Rex, M.A., 1981. Community Structure in the Deep-Sea Benthos. Annual Review of Ecology and Systematics 12, 331–353. https://doi.org/10.1146/annurev.es.12.110181.001555

Rice, T.K., Schork, N.J., Rao, D.C., 2008. Methods for Handling Multiple Testing, in: Advances in Genetics. Elsevier, pp. 293–308. https://doi.org/10.1016/S0065-2660(07)00412-9

Robert, K., Jones, D.O.B., Roberts, J.M., Huvenne, V.A.I., 2016. Improving predictive mapping of deep-water habitats: Considering multiple model outputs and ensemble techniques. Deep Sea Research Part I: Oceanographic Research Papers 113, 80–89. https://doi.org/10.1016/j.dsr.2016.04.008

Robert, K., Jones, D.O.B., Tyler, P.A., Van Rooij, D., Huvenne, V.A.I., 2015. Finding the hotspots within a biodiversity hotspot: fine-scale biological predictions within a submarine canyon using high-resolution acoustic mapping techniques. Marine Ecology 36, 1256–1276. https://doi.org/10.1111/maec.12228

Roberts, J.M., 2009. Cold-Water corals: the biology and geology of deep-sea coral habitats. Cambridge University Press.

Roberts, J.M., Cairns, S.D., 2014. Cold-water corals in a changing ocean. Current Opinion in Environmental Sustainability 7, 118–126. https://doi.org/10.1016/j.cosust.2014.01.004

Ross, L.K., Ross, R.E., Stewart, H.A., Howell, K.L., 2015. The Influence of Data Resolution on Predicted Distribution and Estimates of Extent of Current Protection of Three 'Listed' Deep-Sea Habitats. PLoS ONE 10, e0140061. https://doi.org/10.1371/journal.pone.0140061

Ross, R.E., Howell, K.L., 2013. Use of predictive habitat modelling to assess the distribution and extent of the current protection of 'listed' deep-sea habitats. Diversity Distrib. 19, 433–445. https://doi.org/10.1111/ddi.12010

Sacchetti, F., Benetti, S., Georgiopoulou, A., Shannon, P.M., O'Reilly, B.M., Dunlop, P., Quinn, R., Ó Cofaigh, C., 2012. Deep-water geomorphology of the glaciated Irish margin from high-resolution marine geophysical data. Marine Geology 291–294, 113–131. https://doi.org/10.1016/j.margeo.2011.11.011

Sato, T., 1996. Type I and Type II Error in Multiple Comparisons. Journal of Psychology 130, 293–302.

Saucier, E.H., France, S.C., Watling, L., 2021. Toward a revision of the bamboo corals: Part 3, deconstructing the Family Isididae. Zootaxa 5047, 247–272. https://doi.org/10.11646/zootaxa.5047.3.2

Saucier, E.H., Sajjadi, A., France, S.C., 2017. A taxonomic review of the genus Acanella (Cnidaria: Octocorallia: Isididae) in the North Atlantic Ocean, with descriptions of two new species. Zootaxa 4323. https://doi.org/10.11646/zootaxa.4323.3.2

Sayago-Gil, M., Durán-Muñoz, P., Javier Murillo, F., Díaz-del-Río, V., Serrano, A., Miguel Fernández-Salas, L., 2012. A Study of Geomorphological Features of the Seabed and the Relationship to Deep-Sea Communities on the Western Slope of Hatton Bank (NE Atlantic Ocean), in: Seafloor Geomorphology as Benthic Habitat. Elsevier, pp. 751–761. https://doi.org/10.1016/B978-0-12-385140-6.00055-4

Schlining, B., Stout, N., 2006. MBARI's Video Annotation and Reference System, in: OCEANS 2006. Presented at the OCEANS 2006, IEEE, Boston, MA, USA, pp. 1–5. https://doi.org/10.1109/OCEANS.2006.306879

Shelmerdine, R.L., Shucksmith, R.J., 2015. Understanding the effect of scale and resolution on predictive habitat maps.

Stolar, J., Nielsen, S.E., 2015. Accounting for spatially biased sampling effort in presence-only species distribution modelling. Diversity and Distributions 21, 595–608. https://doi.org/10.1111/ddi.12279

Sundahl, H., Buhl-Mortensen, P., Buhl-Mortensen, L., 2020. Distribution and Suitable Habitat of the Cold-Water Corals Lophelia pertusa, Paragorgia arborea, and Primnoa resedaeformis on the Norwegian Continental Shelf. Front. Mar. Sci. 7, 213. https://doi.org/10.3389/fmars.2020.00213

Sward, D., Monk, J., Barrett, N., 2019. A Systematic Review of Remotely Operated Vehicle Surveys for Visually Assessing Fish Assemblages. Front. Mar. Sci. 6, 134. https://doi.org/10.3389/fmars.2019.00134

Syfert, M.M., Smith, M.J., Coomes, D.A., 2013. The Effects of Sampling Bias and Model Complexity on the Predictive Performance of MaxEnt Species Distribution Models. PLoS ONE 8, e55158. https://doi.org/10.1371/journal.pone.0055158

Thistle, D., Tyler, P.A., 2003. Ecosystems of the Deep Oceans, Ecosystems of the World. Elsevier, Amsterdam 5–39.

Thurber, A.R., Sweetman, A.K., Narayanaswamy, B.E., Jones, D.O.B., Ingels, J., Hansman, R.L., 2014. Ecosystem function and services provided by the deep sea. Biogeosciences 11, 3941–3963. https://doi.org/10.5194/bg-11-3941-2014

UN General Assembly, 2015. Transforming our world: the 2030 Agenda for Sustainable Development.

van Aken, H.M., 2000. The hydrography of the mid-latitude northeast Atlantic Ocean I: The deep water masses.

Vecchione, M., 2019. ROV Observations on Reproduction by Deep-Sea Cephalopods in the Central Pacific Ocean. Front. Mar. Sci. 6, 403. https://doi.org/10.3389/fmars.2019.00403

Walbridge, S., Slocum, N., Pobuda, M., Wright, D., 2018. Unified Geomorphological Analysis Workflows with Benthic Terrain Modeler. Geosciences 8, 94. https://doi.org/10.3390/geosciences8030094

Watling, L., France, S.C., Pante, E., Simpson, A., 2011. Biology of Deep-Water Octocorals, in: Advances in Marine Biology. Elsevier, pp. 41–122. https://doi.org/10.1016/B978-0-12-385529-9.00002-0

Watling, L., Saucier, E.H., Scott, C.F., 2022. Towards a revision of the bamboo corals (Octocorallia): Part 4, delineating the family Keratoisididae. Zootaxa 5093, 337–375.

Weiss, A., 2001. Topographic position and landforms analysis. In *Poster presentation, ESRI user conference,* San Diego, CA (Vol. 200).

Weisstein, E.W., 2004. Bonferroni Correction [WWW Document]. URL https://mathworld.wolfram.com/ (accessed 11.6.23).

Whickam, H., Winston, C., Wickham, M.H., 2016. Package 'ggplot2'. Create elegant data visualisations using the grammar graphics. Version 2.1, 1–189.

Winship, A.J., Thorson, J.T., Clarke, M.E., Coleman, H.M., Costa, B., Georgian, S.E., Gillett, D., Grüss, A., Henderson, M.J., Hourigan, T.F., Huff, D.D., Kreidler, N., Pirtle, J.L., Olson, J.V., Poti, M., Rooper, C.N., Sigler, M.F., Viehman, S., Whitmire, C.E., 2020. Good Practices for Species Distribution Modeling of Deep-Sea Corals and Sponges for Resource Management: Data Collection, Analysis, Validation, and Communication. Front. Mar. Sci. 7, 303. https://doi.org/10.3389/fmars.2020.00303

Wolff, T., 1977. Diversity and faunal composition of the deep-sea benthos. Nature 267, 780–785. https://doi.org/10.1038/267780a0

Wood, S.N., 2017. Generalized additive models: an introduction with R, Second edition. ed. CRC Press/Taylor & Francis Group, Boca Raton.

Wright, D.J., Miller, J., Larkin, E.M., Rinehart, R., Naar, D.F., Donahue, B.T., Anderson, S.M., Battista, T., Lundblad, E.R., 2006. A Benthic Terrain Classification Scheme for American Samoa. Marine Geodesy 29, 89–111. https://doi.org/10.1080/01490410600738021

Yesson, C., Taylor, M.L., Tittensor, D.P., Davies, A.J., Guinotte, J., Baco, A., Black, J., Hall-Spencer, J.M., Rogers, A.D., 2012. Global habitat suitability of cold-water octocorals. Journal of Biogeography 39, 1278–1292. https://doi.org/10.1111/j.1365-2699.2011.02681.x